Physics Letters B 846 (2023) 138223

Contents lists available at ScienceDirect

Physics Letters B

journal homepage: www.elsevier.com/locate/physletb

Evidence of off-shell Higgs boson production from ZZ leptonic decay channels and constraints on its total width with the ATLAS detector

The ATLAS Collaboration *

ARTICLE INFO

Article history:
Received 5 April 2023
Received in revised form 27 September 2023
Accepted 28 September 2023
Available online 5 October 2023
Editor: M. Doser

Dataset link: https://hepdata.cedar.ac.uk

ABSTRACT

This Letter reports on a search for off-shell production of the Higgs boson using 139 fb^{-1} of pp collision data at $\sqrt{s} = 13$ TeV collected by the ATLAS detector at the Large Hadron Collider. The signature is a pair of Z bosons, with contributions from both the production and subsequent decay of a virtual Higgs boson and the interference of that process with other processes. The two observable final states are $ZZ \to 4\ell$ and $ZZ \to 2\ell 2\nu$ with $\ell = e$ or μ. In the $ZZ \to 4\ell$ final state, a dense Neural Network is used to enhance analysis sensitivity with respect to matrix element-based discrimination. The background-only hypothesis is rejected with an observed (expected) significance of 3.3 (2.2) standard deviations, representing experimental evidence for off-shell Higgs boson production. Assuming that no new particles enter the production of the virtual Higgs boson, its total width can be deduced from the measurement of its off-shell production cross-section. The measured total width of the Higgs boson is $4.5^{+3.3}_{-2.5}$ MeV, and the observed (expected) upper limit on the total width is found to be 10.5 (10.9) MeV at 95% confidence level.

1. Introduction

The discovery of the Higgs boson in 2012 by the ATLAS and CMS collaborations at the Large Hadron Collider (LHC) [1,2] was a major milestone in particle physics, and since then this particle has been put under the spotlight for further scrutiny to uncover its fundamental nature. Great progress has been made in measuring the properties and couplings of the Higgs boson [3,4], and to date no deviations from the Standard Model (SM) predictions have been found. The total width of the Higgs boson (Γ_H) is a key prediction of the SM. The expected value in the SM (Γ_H^{SM}) for a 125 GeV Higgs boson is only 4.1 MeV [5], which is inaccessible via any direct measurement of the width in the resonance region due to limited detector resolution. To probe this parameter, a method relying on both off-shell and on-shell production of the Higgs boson has been developed, as documented in [6–9]. In this method, the relationship between the Higgs boson coupling constants in the on-shell and off-shell regimes is assumed to be given by the SM prediction, assuming that no new particles enter into the Higgs boson production process. On-shell Higgs boson production (only gluon-gluon fusion (ggF) is considered in the equations below, but the principle is the same in other production modes) is inversely proportional to the width:

$$\sigma^{\text{on-shell}}_{gg\to H\to ZZ} \sim \frac{g^2_{\text{ggF}} g^2_{\text{HZZ}}}{m_H \Gamma_H}.$$

However, off-shell Higgs boson production has no width dependence:

$$\sigma^{\text{off-shell}}_{gg\to H\to ZZ} \sim \frac{g^2_{\text{ggF}} g^2_{\text{HZZ}}}{m^2_{ZZ}}.$$

Therefore, if the HZZ and effective ggH couplings in the two regimes (where the effective coupling is obtained by treating the quark loop as a single vertex) have a known relationship, Γ_H can be extracted from the ratio of yields of observed Higgs boson events. Off-shell production is accessible in the ZZ decay channel because the available phase space for the decay increases rapidly as the off-shell mass approaches the $2m_Z$ threshold, counteracting the expected drop in the production at higher masses [10–22], where m_Z is the mass of the Z boson.

Multiple searches for off-shell Higgs boson production have been carried out by the ATLAS and CMS collaborations using LHC Run 1 and Run 2 data [23–29]. In practice the signal of off-shell Higgs boson production is a deficit in $gg \to ZZ$ or electroweak $q\bar{q} \to ZZ$ production, due to the negative interference between the off-shell Higgs boson process and the continuum background. Throughout this Letter, the notation $gg \to (H^* \to)ZZ$ is used to refer to the inclusive process that combines the Higgs boson signal $gg \to H^* \to ZZ$, the continuum background process $gg \to ZZ$, and their interference. Similarly, the notation $q\bar{q} \to (H^* \to)ZZ + 2j$

---

* *E-mail address:* atlas.publications@cern.ch.

https://doi.org/10.1016/j.physletb.2023.138223
0370-2693/

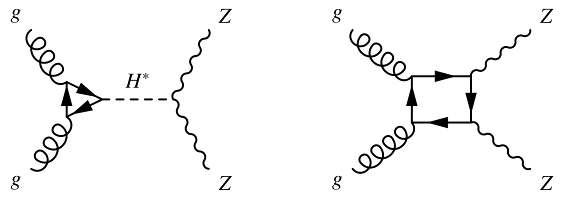

(a) (b)

Fig. 1. The leading-order Feynman diagrams for the (a) $gg \to H^* \to ZZ$ signal and (b) background processes. In the signal process the quark loop is dominated by top and bottom, while for the continuum background it is mainly light quarks.

refers to the inclusive electroweak process that combines the processes $q\bar{q} \to H^* \to ZZ + 2j$, $q\bar{q} \to ZZ + 2j$, and their interference.

The corresponding leading-order Feynman diagrams for the signal and background processes are shown in Figs. 1 and 2. Owing to the clean signature and accessible branching fractions, the four-lepton final states (4ℓ and $2\ell 2\nu$ with $\ell = e$ or μ), originating from the decays of a pair of on-shell Z bosons induced by a virtual Higgs boson, offer the main signal sensitivity. The latest CMS search [29], using 138 fb^{-1} in the $2\ell 2\nu$ channel and 78 fb^{-1} in the 4ℓ channel, led to an observed (expected) detection significance of about 3.6σ (2.4) standard deviations (σ) for off-shell Higgs boson production and a measured Γ_H of $3.2^{+2.4}_{-1.7}$ MeV. The analysis described in this Letter updates the previous ATLAS result [27] with more data – the full Run-2 dataset is used in both decay channels – a more powerful discriminant in the 4ℓ channel, and a data-driven approach to estimating the leading $q\bar{q} \to ZZ$ background. Additionally, in this analysis for the first time ggF and EW off-shell production are probed separately as well as together.

This Letter presents a search for off-shell Higgs boson production in four-lepton final states using the full Run 2 data at a centre-of-mass energy $\sqrt{s} = 13$ TeV collected by the ATLAS detector. Two decay channels, 4ℓ and $2\ell 2\nu$, are separately analysed and then combined to obtain the final results. Events with a pair of Z bosons are categorised into several signal regions (SRs) to probe off-shell contributions from the two leading production modes, ggF and electroweak production (EW), and their respective interference with the continuum background $gg \to ZZ$ and electroweak $q\bar{q} \to ZZ + 2j$ processes. Electroweak production includes the contributions from vector-boson fusion (VBF) and vector-boson associated production (VH), since these two processes both interfere with the electroweak $q\bar{q} \to ZZ + 2j$ background and hence cannot be separated. The main irreducible background is Z boson pair production via quark–antiquark annihilation ($q\bar{q} \to ZZ$); the interfering backgrounds described above also contribute. In the 4ℓ channel, these are the only significant backgrounds, with sub-percent-level contributions from the production of Z bosons with associated jets and $t\bar{t}$ production. In the $2\ell 2\nu$ channel, background processes from diboson production (both WZ and WW), $t\bar{t}$ and single top production, and the production of Z bosons with associated jets constitute roughly half of the total background. Control regions (CRs) are defined to ensure control of the background modelling. In both channels, the background from the combination of vector-boson associated production to a top-quark pair ($t\bar{t} + V$, $V = W$ or Z) and triboson production (ZZZ, WZZ, or WWZ) is at the percent level. Distributions of discriminating variables are fitted simultaneously in all SRs to extract the off-shell contribution by measuring the signal strength $\mu_{\text{off-shell}}$, the off-shell production cross-section normalised to the SM prediction, with the CRs also included in the fit to constrain the normalisation of the main background processes. In the 4ℓ channel, an observable is constructed from the output of neural networks (NN) that are trained with kinematic variables and matrix-element discriminants sensitive to the signal process (see Ref. [27]). The $2\ell 2\nu$ channel uses the transverse mass of the ZZ system,

$$m_{\mathrm{T}}^{ZZ} \equiv \sqrt{\left[\sqrt{m_Z^2 + \left(p_{\mathrm{T}}^{\ell\ell}\right)^2} + \sqrt{m_Z^2 + \left(E_{\mathrm{T}}^{\text{miss}}\right)^2}\,\right]^2 - \left|\vec{p}_{\mathrm{T}}^{\,\ell\ell} + \vec{E}_{\mathrm{T}}^{\text{miss}}\right|^2}, \tag{1}$$

where m_Z is the Z boson mass [30], $\vec{p}_{\mathrm{T}}^{\,\ell\ell}$ and $\vec{E}_{\mathrm{T}}^{\text{miss}}$ are the transverse momentum vector of the lepton pair and the missing transverse momentum vector with magnitudes of $p_{\mathrm{T}}^{\ell\ell}$ and $E_{\mathrm{T}}^{\text{miss}}$, respectively. Finally, the constraint on Γ_H is derived by using both the measured $\mu_{\text{off-shell}}$ and the signal strength for on-shell Higgs boson contributions ($\mu_{\text{on-shell}}$) in the 4ℓ channel obtained from Ref. [31], relying on the equation (valid under the assumptions discussed above) $\mu_{\text{off-shell}}/\mu_{\text{on-shell}} = \Gamma_H/\Gamma_H^{\text{SM}}$. Similarly to the previous ATLAS paper [27], this search also reports the ratio of effective Higgs boson–gluon couplings (R_{gg}) and the ratio of Higgs boson and vector-boson couplings (R_{VV}) between the off-shell and on-shell regions, assuming that the Higgs boson total width takes its SM value.

2. ATLAS detector

ATLAS is a multipurpose detector with a forward–backward symmetric cylindrical geometry and a solid-angle[1] coverage of nearly 4π, described in detail in Ref. [32]. The inner tracking detector (ID), covering the region $|\eta| < 2.5$, consists of a silicon pixel detector, a silicon microstrip detector, and a transition-radiation tracker. The innermost layer of the pixel detector, the insertable B-layer [33], was installed between Run 1 and Run 2 of the LHC. The inner detector is surrounded by a thin superconducting solenoid providing a 2 T magnetic field, and by a finely segmented lead/liquid-argon (LAr) electromagnetic calorimeter covering the region $|\eta| < 3.2$. A steel/scintillator-tile hadron calorimeter provides coverage in the central region $|\eta| < 1.7$. The endcap and forward regions, covering the pseudorapidity range $1.5 < |\eta| < 4.9$, are instrumented with LAr electromagnetic and hadron calorimeters, with steel, copper, or tungsten as the absorber material. A muon spectrometer (MS) system incorporating large superconducting toroidal air-core magnets surrounds the calorimeters. Three layers of precision wire chambers provide muon tracking in the range of $|\eta| < 2.7$, while dedicated fast chambers are used for triggering in the region $|\eta| < 2.4$. The trigger system, composed of two stages, was upgraded [34] before Run 2. The first stage, implemented with custom hardware, uses information from the calorimeters and muon chambers to select events from the 40 MHz bunch crossings at a maximum rate of 100 kHz. The second stage, called the high-level trigger (HLT), reduces the data acquisition rate to about 1 kHz on average. The HLT is software-based and runs reconstruction algorithms similar to those used in offline reconstruction. An extensive software suite [35] is used in data simulation, in reconstruction and analysis of real and simulated data, in detector operations, and in the trigger and data acquisition systems of the experiment.

---

[1] The ATLAS experiment uses a right-handed coordinate system with its origin at the nominal interaction point (IP) in the centre of the detector and the z-axis along the beam pipe. The x-axis points from the IP to the centre of the LHC ring, and the y-axis points upward. Cylindrical coordinates (r, ϕ) are used in the transverse plane, ϕ being the azimuthal angle around the z-axis. The pseudorapidity is defined in terms of the polar angle θ as $\eta = -\ln\tan(\theta/2)$.

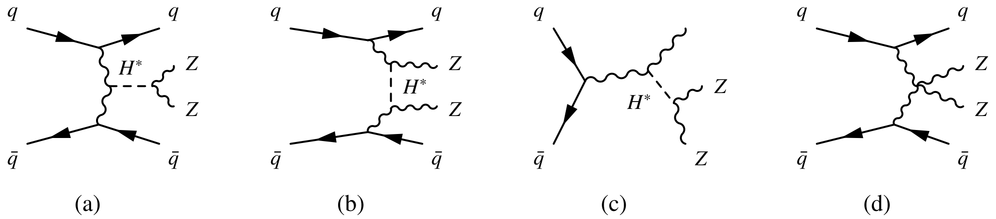

Fig. 2. The leading-order Feynman diagrams for (a) the *s*-channel vector-boson fusion signal, (b) the *t*-channel vector-boson fusion signal, (c) the vector-boson associated production signal, and (d) the vector-boson scattering background.

3. Data and Monte Carlo simulation

The proton–proton (pp) collision data used in this search were collected from 2015 to 2018, corresponding to an integrated luminosity of 139 fb^{-1}. Events in the 4ℓ final state were recorded with a combination of single-lepton, dilepton and trilepton triggers, while the $2\ell2\nu$ events were collected via multiple single-lepton triggers. The overall trigger efficiency for the off-shell signal process is more than 98% in each final state after the application of the SR selections defined below.

Monte Carlo (MC) simulation is used to predict the normalisation and event kinematics of the signal process and some of the backgrounds. Event samples for each process were first produced by a corresponding event generator and then passed through detector simulation [36] within the GEANT4 framework [37]. Additional inelastic pp interactions (pile-up) modelled with PYTHIA8.186 [38] were overlaid on the simulated events to mimic the real collision events, and further corrections were applied to the simulated samples to match the pile-up conditions in the data. The lepton and jet momentum scale and resolution, and the lepton reconstruction, identification, isolation and trigger efficiencies in the simulation were corrected to match those measured in data.

Separate simulated samples were generated for each of the off-shell signal from ggF production, the $gg \to ZZ$ background, and the inclusive production $gg \to (H^* \to)ZZ$, which also includes the interference between the two. These loop-induced processes were modelled by SHERPA v2.2.2 [39] with OPENLOOPS [40–42] at leading-order (LO) accuracy in quantum chromodynamics (QCD), with up to one additional parton in the final state, using the NNPDF3.0 parton distribution function (PDF) set [43]. Signal and background were simulated separately from the inclusive process for NN training and template fitting. The merging with the parton shower was performed using the MEPS@NLO prescription [44] and the SHERPA built-in algorithm was used for parton showering and hadronisation. The samples are corrected to next-to-leading order (NLO) in QCD using corrections calculated separately as a function of the invariant mass of the ZZ system (m_{ZZ}) [45,46] for the signal, background, and inclusive processes. These corrections are similar for each process and range from 1.5 to 2. The total normalisation of all three processes was then corrected to next-to-next-to-next-to-leading order (N3LO) in QCD using a constant correction of 1.32, derived for the off-shell signal [47,48]. The use of the same correction for all processes is justified as the N3LO corrections are expected to be very similar for signal, background, and interference [49,50].

EW production of ZZ and two jets, also denoted by $q\bar{q} \to (H^* \to)\ ZZ + 2j$, contains inclusively the off-shell signal from VBF production, VH production, the non-Higgs boson EW $ZZjj$ process, and their interferences. Those processes were modelled by MADGRAPH5_AMC@NLO [51] at LO QCD accuracy using the NNPDF3.0 NLO PDF set [52]. PYTHIA8.244 [38] was used for parton showering and hadronisation with the A14 set of tuned parameters (tune) for the underlying event [53]. The t-channel exchange of the Higgs boson is treated as a contribution to the VBF signal process.

The ggF- and VBF-induced contributions can be straightforwardly parameterised as a function of $\mu_{\text{off-shell}}$, where the off-shell signal and the interference depend on $\mu_{\text{off-shell}}$ and $\sqrt{\mu_{\text{off-shell}}}$, respectively. More details of this parameterisation are given in Section 8.

The $q\bar{q} \to ZZ$ background was simulated by SHERPA v2.2.2 with OPENLOOPS using the NNPDF3.0 NNLO PDF set. The matrix elements were calculated to NLO accuracy in QCD for 0- and 1-jet final states, and to LO accuracy for 2- and 3-jet final states. The merging with the SHERPA parton shower was performed using the MEPS@NLO prescription [54]. NLO EW corrections calculated on top of the LO QCD prediction were applied as a function of m_{ZZ} for the 4ℓ final state [55,56], while the m_{ZZ}-based corrections for the $2\ell2\nu$ channel were averaged from the additive (NLO EW + NLO QCD) and multiplicative (NLO EW × NLO QCD) approaches following Ref. [57]. A cross-check was performed in the 4ℓ channel, and the results of the two approaches were found to agree within their uncertainties, while the uncertainties of both approaches (described in detail below) were also found to be similar.

The WZ diboson events from both QCD and EW production, with the subsequent leptonic decays of both the W and Z bosons, were simulated using SHERPA with a similar set-up to that of the $q\bar{q} \to ZZ$ background. The WZ events with the Z boson decaying leptonically and the W boson decaying hadronically were modelled with SHERPA v2.2.1. For the $2\ell2\nu$ final state, the contribution from WW production was removed in the SHERPA simulation of the $q\bar{q} \to ZZ$ and $gg \to ZZ$ processes by requiring the charged leptons and the neutrinos to have different lepton flavours (the prediction was then scaled up by 1.5 to compensate). The $q\bar{q} \to WW$ and $gg \to WW$ processes were then modelled with POWHEG BOX v2 [58] and SHERPA v2.2.2, respectively. The interference between WW and ZZ production in the $2\ell2\nu$ final state is expected to be negligible in the phase space of the analysis [57] and was therefore not considered.

The Z+jets background was simulated using the SHERPA v2.2.1 event generator, where the matrix elements were calculated for up to two partons at NLO and four partons at LO. The Z+jets events were normalised using the NNLO cross-sections [59]. The $t\bar{t}$ background, as well as single-top (including s-channel, t-channel, and the dominant Wt component) production, were modelled using POWHEG BOXv2 interfaced to PYTHIA8.230 with the A14 tune. The total cross-sections for $t\bar{t}$ production and single-top production were normalised to the predictions at NNLO and NLO accuracy in QCD [60–62], respectively.

The triboson backgrounds ZZZ, WZZ, and WWZ with fully leptonic decays were modelled with SHERPA v2.2.2 at NLO QCD accuracy. The $ZZZ \to 4\ell + 2j$ process is included in the $q\bar{q} \to (H^* \to)\ ZZ + 2j$ sample described above. The simulation of $t\bar{t} + V$ production ($V = W$ or Z) with at least one of the top quark decaying leptonically and the vector boson decaying inclusively was performed with MADGRAPH5_AMC@NLO interfaced to PYTHIA8.210 for parton showering and hadronisation with the A14 tune. The total cross-sections for the $t\bar{t} + V$ backgrounds were normalised to the NLO QCD and EW predictions from Ref. [63].

4. Reconstruction of physics objects

To describe the event signature and obtain a good signal-to-background ratio, this search relies on the successful reconstruction of collision vertices, electrons, muons, jets, $\vec{E}_{\mathrm{T}}^{\mathrm{miss}}$, as well as identification of jets containing b-hadrons (b-jets). The reconstruction is identical to that in Ref. [64], and briefly summarised as follows.

Events are first required to have a collision vertex associated with at least two tracks each with transverse momentum $p_{\mathrm{T}} > 0.5$ GeV. The vertex with the highest sum of p_{T}^2 of the associated tracks is referred to as the primary vertex.

Muons are primarily identified by tracks or segments (tracks using the hits of a single MS station) reconstructed in the MS and matched to tracks reconstructed in the ID, with exceptions in areas where the MS lacks coverage. In the region $2.5 < |\eta| < 2.7$, muons can also be identified by tracks from the muon spectrometer alone (standalone muons). In the gap region ($|\eta| < 0.1$) of the MS, muons can be identified by a track from the ID associated with a compatible calorimeter energy deposit (calorimeter-tagged muons). Candidate muons are required to have $p_{\mathrm{T}} > 5$ GeV and $|\eta| < 2.7$, with the exception of calorimeter-tagged muons for which the p_{T} threshold is raised to 15 GeV. Muons must satisfy the 'loose' identification criterion [65] in the 4ℓ channel with at most one standalone or calorimeter-tagged muon allowed per Higgs boson candidate. In the $2\ell 2\nu$ channel muons are selected with $|\eta| < 2.5$ and must satisfy the 'medium' identification criterion. Electrons are reconstructed from energy deposits in the electromagnetic calorimeter matched to a track in the ID. Candidate electrons must have $p_{\mathrm{T}} > 7$ GeV and $|\eta| < 2.47$, and satisfy the 'loose' and 'medium' identification criteria [66] in the 4ℓ and $2\ell 2\nu$ channels, respectively. All electrons and muons used in both channels must be isolated and satisfy the 'FixedCutPFlowLoose' isolation criteria [65,66]. Furthermore, electrons (muons) are required to have associated tracks satisfying $|d_0/\sigma_{d_0}| < 5$ (3) and $|z_0 \times \sin\theta| < 0.5$ mm, where d_0 is the transverse impact parameter relative to the beam line, σ_{d_0} is its uncertainty, and z_0 is the z coordinate of the r-ϕ impact point, defined relative to the primary vertex. The event is rejected if the minimum angular separation between two leptons is $\Delta R_{\ell\ell} < 0.1$, where $\Delta R_{\ell\ell} = \sqrt{(\Delta\phi_{\ell\ell})^2 + (\Delta\eta_{\ell\ell})^2}$.

Jets are reconstructed from particle-flow objects [67] using the anti-k_t algorithm [68,69] with radius parameter $R = 0.4$. The jet-energy scale is calibrated using simulation and further corrected with in situ methods [70]. Candidate jets are required to have $p_{\mathrm{T}} > 30$ GeV and $|\eta| < 4.5$. A jet-vertex tagger [71] is applied to jets with $p_{\mathrm{T}} < 60$ GeV and $|\eta| < 2.4$ to suppress jets that originate from pile-up. To mitigate the impact of pile-up jets in the forward region, another tagger, based on jet shapes and topological jet correlations [72], is used to suppress jets originating from the pile-up with $p_{\mathrm{T}} < 50$ GeV and $2.5 < |\eta| < 4.5$. In addition, b-jets are identified using a multivariate b-tagging algorithm [73] and events containing them are rejected. The chosen b-tagging algorithm has an efficiency of 85% for b-jets and a rejection factor of 33 against light-flavour jets, measured in $t\bar{t}$ events [74].

The presence of neutrinos is identified using the missing transverse momentum vector $\vec{E}_{\mathrm{T}}^{\mathrm{miss}}$, which is computed as the opposite of the vector sum of transverse momenta of all the leptons and jets, as well as the tracks originating from the primary vertex but not associated with any of the leptons or jets [75]. Missing transverse momentum may also arise from the mismeasurement of the momentum of particles or jets. To avoid accepting events due to the presence of this kind of fake $E_{\mathrm{T}}^{\mathrm{miss}}$, the statistical significance of the $E_{\mathrm{T}}^{\mathrm{miss}}$, S($E_{\mathrm{T}}^{\mathrm{miss}}$), is used. S($E_{\mathrm{T}}^{\mathrm{miss}}$) is calculated from the resolution information of the physics objects used in the $E_{\mathrm{T}}^{\mathrm{miss}}$ reconstruction [76].

5. $ZZ \to 4\ell$ analysis

The selection of candidate events used in the signal and control regions of the 4ℓ channel closely follows that described in Ref [64]. The four-lepton invariant mass is required to be above the on-shell ZZ production threshold, $m_{4\ell} > 180$ GeV. Candidate 4ℓ quadruplets are formed by selecting two opposite-sign, same-flavour dilepton pairs in each event. In the 4e and 4μ channels, in which there are two possible pairings, the one that includes the lepton pair with mass closest to the Z boson mass is chosen. The p_{T} thresholds for the three leading leptons are 20, 15 and 10 GeV, respectively. In each quadruplet, the lepton pair with mass closest to the Z boson mass, m_{12}, is referred to as the leading pair and required to have $50 < m_{12} < 106$ GeV. The sub-leading pair, m_{34}, must satisfy $50 < m_{34} < 115$ GeV when $m_{4\ell} > 190$ GeV. Due to the increased probability of one off-shell Z boson at lower values of $m_{4\ell}$, the lower threshold for m_{34} decreases linearly to 45 GeV for $180 < m_{4\ell} < 190$ GeV.

Three SRs are designed to provide sensitivity to both the EW and ggF production modes. The SRs are defined such that $m_{4\ell}$ is well above the Higgs boson mass, including only events with $m_{4\ell} > 220$ GeV. Events in the range $180 < m_{4\ell} < 220$ GeV are expected to have the lowest signal-to-background ratio in the $m_{4\ell}$ range of the analysis and so are reserved for the control regions defined below. Events containing two or more jets with p_{T} greater than 30 GeV, where the two leading jets are well separated in η, $|\Delta\eta_{\mathrm{jj}}| > 4$, are classified into the EW SR. Events falling outside the EW SR but featuring exactly one jet in the forward direction ($|\eta_j| > 2.2$) are assigned to a mixed SR. All the remaining events are then assigned to the ggF SR.

The main background in the 4ℓ channel is the $q\bar{q} \to ZZ$ process. The overall normalisation of this background is constrained by data in three different CRs defined with $180 < m_{4\ell} < 220$ GeV and with zero, one, or ≥ 2 jets. The signal contamination in these CRs is below 2%. The kinematic distributions are modelled with simulation, described in Section 3. Events in the zero- and one-jet CRs are binned in four and two intervals of equal width in $m_{4\ell}$, respectively, to provide further information about event kinematics. The interfering background processes $gg \to ZZ$ and EW $q\bar{q} \to ZZ$, as well as the small backgrounds from triboson production and $t\bar{t}Z$, are estimated from simulation. The contribution of the reducible backgrounds where hadrons or their decay products are mis-reconstructed as prompt leptons, such as Z+jets, WZ and $t\bar{t}$ processes, are estimated by using data-driven methods described in Ref. [64] and found to be negligible.

To maximise the signal sensitivity, a multi-class dense NN is employed in the SRs to enhance events with a Higgs boson candidate. The NN, implemented using Keras [77] with TensorFlow [78] as the backend, is designed to differentiate among the three event classes: the off-shell Higgs boson signal (S), the interfering background (B), and the non-interfering (NI) background. The interfering backgrounds to the ggF and EW signals are the $gg \to ZZ$ and EW $q\bar{q} \to ZZ + 2j$ processes, respectively. The non-interfering background is the $q\bar{q} \to ZZ$ process in both production modes.

The outputs of the NN use a normalised exponential function so that they can be interpreted as probabilities of an event belonging to a particular class (P_{S}, P_{B} and P_{NI}) and their ratio is used to define the final observable:

$$O_{\mathrm{NN}} = \log_{10}\left(\frac{P_{\mathrm{S}}}{P_{\mathrm{B}} + P_{\mathrm{NI}}}\right).$$

As the analysis attempts to constrain both the ggF- and EW-induced off-shell signals independently, two separate NNs are trained, one in the ggF SR and the other in the EW SR. The observable from the first NN ($O_{\mathrm{NN}}^{\mathrm{ggF}}$) is then used as the discriminating variable in both the ggF and mixed SRs, while that of the second NN ($O_{\mathrm{NN}}^{\mathrm{EW}}$) is used in the EW SR.

The first NN is trained to discriminate among the ggF-induced signal, the $gg \to ZZ$ background, and the $q\bar{q} \to ZZ$ process. The features used by this NN include the kinematic information of the four leptons from MC simulation and also the square of the modulus of the values of the LO matrix element (ME) for the four leptons. The LO MEs are calculated for the gluon-induced signal and background processes and the $q\bar{q} \to ZZ$ process from the final-state variables in the Higgs boson rest frame using the MCFM program [8,27]. The kinematic variables are the leading Z boson production angle and four decay angles defined in Ref [79], and the three invariant masses $m_{4\ell}$, m_{12} and m_{34}. These are used as inputs to the ME calculation, and, along with the transverse momentum of the four-lepton system, as inputs to the NN as well.

The second NN is used to separate the EW-induced off-shell signal process from the non-Higgs boson EW $q\bar{q} \to ZZjj$ background and the QCD-induced $q\bar{q} \to ZZjj$ process. In addition to the variables used in the first NN, with matrix elements calculated specifically for the final state with two jets, several supplementary variables are included to exploit the kinematics of the dijet system: the invariant mass and azimuthal separation of the two leading jets, and the two Zeppenfeld angular variables, calculated for each Z boson as $\eta_{\mathrm{Zep}} = \eta_{Z_1} - (\eta_{j_1} + \eta_{j_2})/2$ [80].

The two networks have 7 and 9 hidden layers respectively, with [90, 80, 80, 75, 75, 40, 40] and [60, 65, 70, 85, 90, 80, 75, 50, 30] neurons. The sparse categorical cross-entropy loss was used to optimise the network structure as well as the learning rate of the Adam optimiser. Input features were chosen to fully describe the event kinematics. The networks were trained on samples of the signal and the interfering and non-interfering backgrounds.

Fig. 3 shows the distributions of the observed and expected NN-based observables in all three signal regions. The data is shown after the simultaneous fit described in Section 8, except that the fit is carried out only in the 4ℓ channel and the value of $\mu_{\text{off-shell}}$ is set equal to one. All systematic uncertainties, which are described in Section 7, are included.

6. $ZZ \to 2\ell 2\nu$ analysis

The $2\ell 2\nu$ final state consists of a pair of isolated leptons (e or μ) and large $E_{\mathrm{T}}^{\mathrm{miss}}$. It has a larger branching fraction than the 4ℓ channel, but is subject to larger background contamination. Candidate events are preselected by requiring exactly two electrons or muons with opposite charges and $p_{\mathrm{T}} > 20$ GeV. The leading lepton must have $p_{\mathrm{T}} > 30$ GeV to surpass the trigger thresholds. To suppress the WZ background, events containing any additional lepton satisfying the loose identification criteria with $p_{\mathrm{T}} > 7$ GeV are rejected. Requiring the dilepton invariant mass ($m_{\ell\ell}$) to be between 76 and 106 GeV largely reduces the contamination from the non-resonant-$\ell\ell$ background, originating from $t\bar{t}$, single-top (dominated by the Wt process), and $q\bar{q} \to WW$ production. Events that satisfy this preselection are then further separated into the SRs and CRs. To suppress the remaining background dominated by the Z + jets and non-resonant-$\ell\ell$ processes, further selections based on $E_{\mathrm{T}}^{\mathrm{miss}}$ and the topology of the candidate events are applied. Candidate events are required to have $E_{\mathrm{T}}^{\mathrm{miss}} > 120$ GeV and $\mathrm{S}(E_{\mathrm{T}}^{\mathrm{miss}}) > 10$. The azimuthal-angle difference between the dilepton system and $\vec{E}_{\mathrm{T}}^{\mathrm{miss}}$, $\Delta\phi(\vec{p}_{\mathrm{T}}^{\,\ell\ell}, \vec{E}_{\mathrm{T}}^{\mathrm{miss}})$, must be larger than 2.5 radians, and the selected leptons must be close to each other, with the distance $\Delta R_{\ell\ell}$ below 1.8. Furthermore, the azimuthal-angle difference between any of the selected jets with $p_{\mathrm{T}} > 100$ GeV and $\vec{E}_{\mathrm{T}}^{\mathrm{miss}}$ must be larger than 0.4 radians to suppress events with poorly measured jet energies. Finally, events containing one or more b-jets are rejected to further suppress the $t\bar{t}$ and Wt backgrounds. The selected events are then categorised into three SRs in the same way as for the 4ℓ channel.

The shape and normalisation of the main background contribution from $q\bar{q} \to ZZ$ production are estimated from simulation, while in the combined result the overall normalisation factors are constrained by the ZZ CRs defined in the 4ℓ channel as described in the previous section. As is shown later in Table 4, the measured normalisations generally agree fairly well with the simulated ones, so this is a safe approach for developing the analysis in this final state.

To estimate the background from WZ production, control regions enriched in WZ events, with a purity of over 90%, are defined using the full event selection given above, except that the presence of a third lepton with $p_{\mathrm{T}} > 20$ GeV is required. Several further selections such as $\mathrm{S}(E_{\mathrm{T}}^{\mathrm{miss}}) > 3$, a b-jet veto, and $m_{\mathrm{T}}^{W} > 60$ GeV, where m_{T}^{W} is constructed from the third lepton's transverse momentum and the $\vec{E}_{\mathrm{T}}^{\mathrm{miss}}$ vector[2], are applied to suppress non-WZ contributions. Three separate WZ CRs are defined according to the number of jets (zero, one, and ≥ 2 jets), and the CRs are included in the statistical fit to separately constrain the normalisation of the WZ background in each N_{jets} bin. The shapes of the kinematic distributions are estimated from simulation.

To estimate the non-resonant-$\ell\ell$ background, arising from $qq \to WW$, $t\bar{t}$, and single-top production, a control region dominated by the non-resonant-$\ell\ell$ processes (with a purity of about 95%) is defined with all the event selection criteria except that the final state is required to contain an opposite-sign $e\mu$ pair. The non-resonant-$\ell\ell$ contribution with the ee ($\mu\mu$) pair is quite similar to that with the $e\mu$ pair, and the difference in lepton reconstruction is taken into account in the simulation. This CR is then used to constrain the total normalisation of the non-resonant-$\ell\ell$ background in all three SRs, and the kinematic shapes are modelled with simulation. The Z + jets background contribution is estimated from simulation and constrained by a normalisation factor derived in a control region enriched in Z + jets events. The control region is defined with all event selection criteria except that $\mathrm{S}(E_{\mathrm{T}}^{\mathrm{miss}})$ is required to be less than 9, and no requirements on the azimuthal angle difference between jets with $p_{\mathrm{T}} > 100$ GeV and $\vec{E}_{\mathrm{T}}^{\mathrm{miss}}$ are made. The resulting control region is about 73% pure. The kinematic distributions for the Z + jets background are modelled with simulation. The CRs for the non-resonant-$\ell\ell$ and the Z + jets backgrounds are not further divided to match the categorisation of SRs depending on jet multiplicity, due to insufficient events in the data. Finally, minor backgrounds from the VVV and $t\bar{t}V$ processes are estimated from simulation.

The distributions of the final observable m_{T}^{ZZ} in the $2\ell 2\nu$ channel, as defined in Eq. (1), are presented in Fig. 4. The data is shown after the simultaneous fit described in Section 8, except that the fit is carried out only in the $2\ell 2\nu$ channel and the value of $\mu_{\text{off-shell}}$ is set equal to one. All three SRs are shown together with the total systematic uncertainty from the sources described in Section 7.

7. Systematic uncertainties

The sources of systematic uncertainty impacting the analysis of both channels can be divided into two categories: uncertainties in the theoretical description of the signal and background processes and experimental uncertainties related to the detector response.

The largest source of systematic uncertainties arises from the theoretical modelling of the signal and background processes, including those related to the production of jets associated with the Higgs boson. Experimental uncertainties related to the reconstruc-

---

[2] $m_{\mathrm{T}}^{W} \equiv \sqrt{2 p_{\mathrm{T}}^{\ell} E_{\mathrm{T}}^{\mathrm{miss}} [1 - \cos\Delta\phi(\vec{p}_{\mathrm{T}}^{\,\ell}, \vec{E}_{\mathrm{T}}^{\mathrm{miss}})]}$.

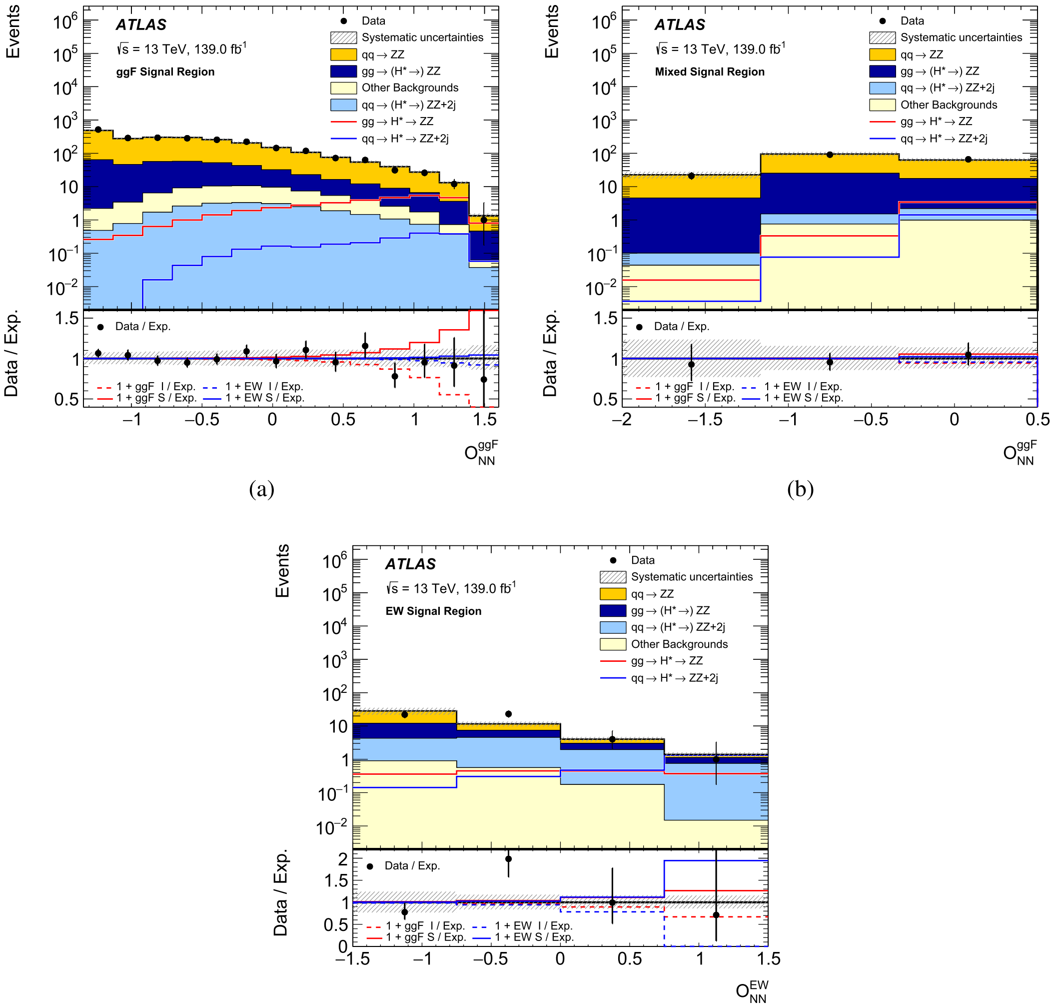

(a)

(b)

(c)

Fig. 3. The observed and expected Standard Model distributions in the 4ℓ channel for (a) $O_{\mathrm{NN}}^{\mathrm{ggF}}$ in the ggF signal region, (b) $O_{\mathrm{NN}}^{\mathrm{ggF}}$ in the mixed signal region, and (c) $O_{\mathrm{NN}}^{\mathrm{EW}}$ in the EW signal region. The observed data are shown following the fit described in Section 8, except that the fit is carried out only in the 4ℓ channel and the off-shell Higgs boson signal is fixed to the SM expectation. The total systematic uncertainty, including all uncertainties described in Section 7, is shown as the hatched area including correlations between uncertainties. The expectation includes the inclusive (signal plus background plus interference) $gg \to (H^* \to)ZZ$ (dark blue) and $q\bar{q} \to (H^* \to)ZZ + 2j$ (light blue) processes, as well as the backgrounds from QCD $q\bar{q} \to ZZ$ production (orange) and other processes (Z+jets, $t\bar{t}$, triboson and $t\bar{t}V$) (yellow). The expected $gg \to H^* \to ZZ$ and EW $q\bar{q} \to H^* \to ZZ + 2j$ signals are also shown as red and blue lines. The first and last bins include the underflow and overflow, respectively. The lower panel of each plot shows the ratio of data to expectation (black points) and the total systematic uncertainty (hatched area), as well as the ratio of the signal (solid lines) and the interference (dashed lines) to the expectation for ggF (red) and EW (blue) production. (For ease of display, for the last four curves one plus the ratio is plotted.)

tion of jets are also prominent while other experimental uncertainties are generally small. To help understand the impact of the leading uncertainties, their relative size before the statistical fit for a specific process is provided in this section, with the largest uncertainties for the main processes in the signal and control regions summarised in Table 1. The impact of these uncertainties on the observed upper limits of $\mu_{\text{off-shell}}$ is given in Section 8.

The theoretical uncertainties arise from the choice of PDF, from the missing higher-order corrections in both QCD and EW perturbative calculations, and from the modelling of the parton shower.

The PDF uncertainties are evaluated using the NNPDF prescription with MC replicas. The PDF covariance matrix between each channel of the analysis is estimated from the 100 replicas from the NNPDF3.0 NNLO set. Only the principal component of the covariance matrix has a non-negligible impact on the yields and it is used as a representation of the PDF uncertainty including its bin-by-bin correlations. The uncertainties due to missing higher-order QCD corrections are estimated by varying the renormalisation and factorisation scales independently, ranging from a factor of one-half to two (excluding the cases in which one scale is varied down by one-half and the other up by two). For the $q\bar{q} \to ZZ$ background, the uncertainty is evaluated independently in bins of N_{jets}. For the gluon-induced processes, including the signal, the $gg \to ZZ$ background, and their interference, the missing higher-order uncertainties are evaluated by their impact on the respective NLO K-factors [81]. The uncertainties are increased in the kinematic regions of the SRs where the K-factor calculations are less precise due to missing effects from on-shell top quarks and high-p_{T} jets [27]: the uncertainty is doubled in the phase space containing a jet with $p_{\mathrm{T}} > 150$ GeV and increased by 50% for m_{ZZ} around twice the top-quark mass. In both the 4ℓ and $2\ell 2\nu$ channels, the uncertainty from missing higher order corrections in the $q\bar{q} \to ZZ$ background is one of the largest uncertainties, ranging from a few percent up to 40% depending on jet multiplicity and observable bin. In both channels, the same uncertainty in the gluon–gluon processes ranges from 10% to 20%.

The uncertainties due to missing higher-order EW corrections (HOEW) are considered for the main $q\bar{q} \to ZZ$ background and handled differently in the two channels. For the $2\ell 2\nu$ channel, the difference in the NLO EW correction between the multiplicative

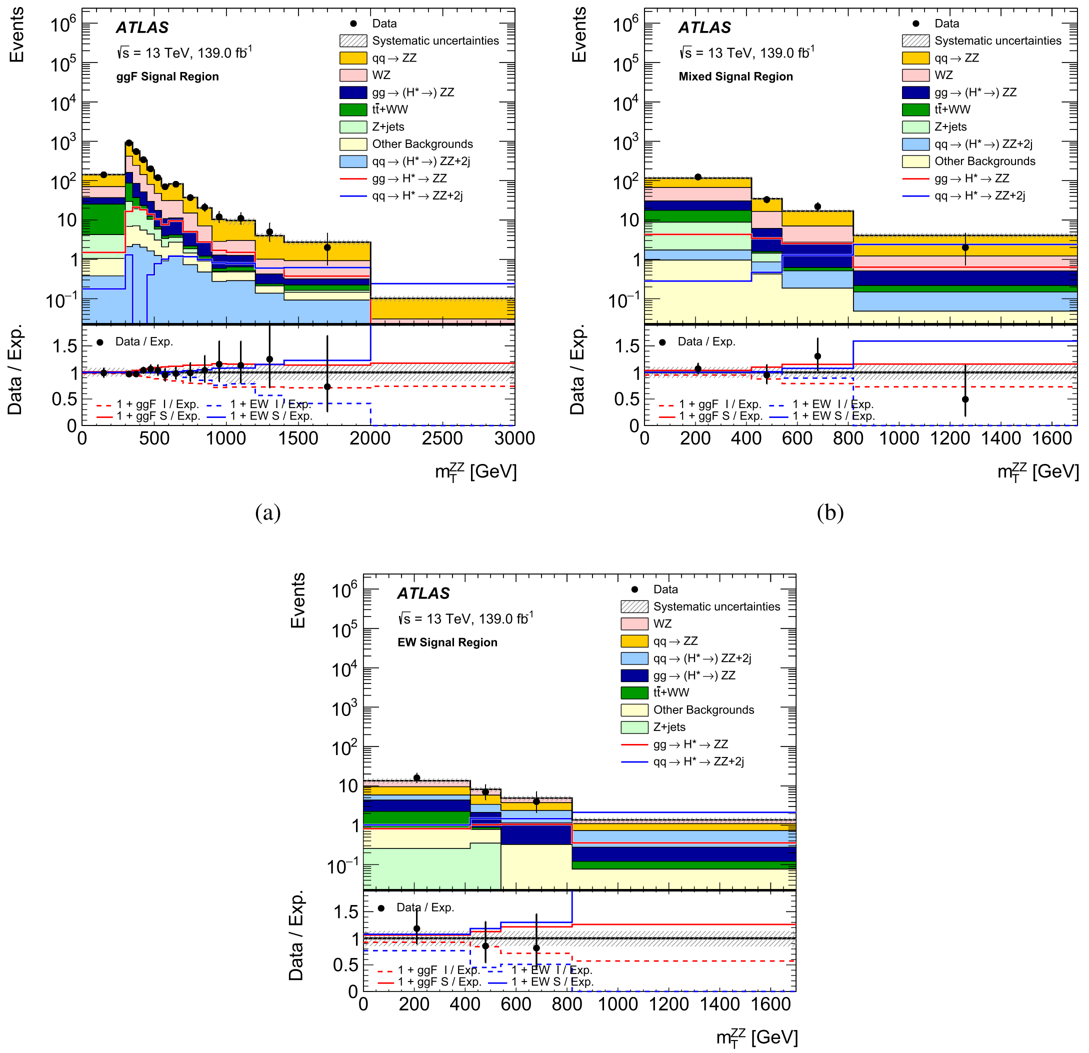

Fig. 4. The observed and expected Standard Model m_T^{ZZ} distributions in the $2\ell 2\nu$ channel for (a) the ggF SR, (b) the mixed SR, and (c) the EW SR. The data are shown after the simultaneous fit described in Section 8, except that the fit is carried out only in the $2\ell 2\nu$ channel and the off-shell Higgs boson signal is fixed to the SM expectation. The hatched area shows the total systematic uncertainty after the fit, comprising all uncertainties described in Section 7 and including correlations between uncertainties. The expectation includes the inclusive (signal plus background plus interference) $gg \to (H^* \to)ZZ$ (dark blue) and EW $q\bar{q} \to (H^* \to)ZZ + 2j$ (light blue) production, as well as the backgrounds from QCD $q\bar{q} \to ZZ$ production (orange), WZ (pink), non-resonant $\ell\ell$ (dark green), Z+jets (light green), and other (triboson and $t\bar{t}V$) (yellow) processes. The expected $gg \to H^* \to ZZ$ and $q\bar{q} \to H^* \to ZZ + 2j$ signals are also shown as red and blue lines. The last bins include the overflow. The lower panel shows the ratio of data to expectation (black points) and the total systematic uncertainty (hatched area), as well as the ratio of the signal (solid lines) and the interference (dashed lines) to the expectation for ggF (red) and EW (blue) production. (For ease of display, for the last four curves one plus the ratio is plotted.)

and additive methods as a function of m_{ZZ} is assigned as the uncertainty [57]. This uncertainty ranges from 1% to at most 20% of the cross-section depending on the bins of observables. For the 4ℓ channel, the NLO EW corrections are calculated on top of the LO QCD cross-section. Therefore, a specific prescription [82], also applied in Ref. [27], is used to derive the uncertainty to account for missing NLO QCD+EW diagrams. A study of the compatibility between the two methods in the 4ℓ channel shows that the central values agree to within a few percent while the uncertainties have a similar size.

The uncertainties due to the modelling of the parton shower and hadronisation play an important role in this search, as jet multiplicity, a key variable used to define both the SRs and the CRs, is particularly sensitive to the modelling of matrix elements, parton showering, and the merging and matching between the two. The parton shower (PS) uncertainties are evaluated by varying resummation and matching scales for the processes simulated with the Sherpa generator. These variations for Sherpa samples are expected to further account for the shape uncertainties relating to missing high-order QCD effects beyond those from the usual QCD scale variations, i.e. migrations between jet bins. For those processes simulated with the Pythia shower program, the uncertainty is assessed by varying the Pythia configurations, such as the parameter values of the A14 tune, the multi-parton models and the final-state radiation models. For ggF production, the PS uncertainties are correlated between the signal and background processes. The uncertainties are split into shape and normalisation components, with the latter being more significant.

In the $2\ell 2\nu$ channel, the systematic uncertainties arising from the PS are parameterised using only the ZZ transverse momentum. In this channel, the PS uncertainty in the ggF processes is quite important: it is about 25% in the yields and ranges from a few percent to a maximum of 15% in the observable shapes. For the EW processes, this uncertainty reaches 15% in the yields and a few percent in the shapes. The PS uncertainties for the $q\bar{q} \to ZZ$ background are at percentage level for the bulk of ob-

Table 1
The dominant uncertainties in the leading processes in the signal and background regions. Uncertainties may depend on the value of the observable: if so, a range is given in the table. Detailed descriptions of the uncertainties are given in the text.

Process	Uncertainty	Final State	Value (%)
ggF Signal Region			
$q\bar{q} \to ZZ$	QCD Scale	$2\ell 2\nu$	4–40
$q\bar{q} \to ZZ$	QCD Scale	4ℓ	21–28
$q\bar{q} \to ZZ$	HOEW	4ℓ	1–7
$q\bar{q} \to ZZ$	HOEW	$2\ell 2\nu$	2–20
$q\bar{q} \to ZZ$	Parton Shower	$2\ell 2\nu$	1–67
$q\bar{q} \to ZZ+2j$	Parton Shower	$2\ell 2\nu$	1–33
$q\bar{q} \to ZZ+2j$	Parton Shower	4ℓ	2–10
$gg \to H^* \to ZZ$	Parton Shower	4ℓ	27
$gg \to H^* \to ZZ$	Parton Shower	$2\ell 2\nu$	8–45
$gg \to ZZ$	Parton Shower	4ℓ	38
$gg \to ZZ$	Parton Shower	$2\ell 2\nu$	6–43
$WZ+0j$	QCD Scale	$2\ell 2\nu$	1–54
1-jet Signal Region			
$gg \to H^* \to ZZ$	Parton Shower	4ℓ	27
$gg \to H^* \to ZZ$	QCD Scale	$2\ell 2\nu$	13–18
$gg \to ZZ$	Parton Shower	4ℓ	38
$gg \to ZZ$	QCD Scale	$2\ell 2\nu$	18–20
$q\bar{q} \to ZZ+2j$	QCD Scale	$2\ell 2\nu$	7–18
$q\bar{q} \to ZZ+2j$	QCD Scale	4ℓ	3–10
2-jet Signal Region			
$q\bar{q} \to ZZ$	QCD Scale	4ℓ	18–26
$q\bar{q} \to ZZ$	QCD Scale	$2\ell 2\nu$	8–32
$gg \to H^* \to ZZ$	Parton Shower	4ℓ	27
$gg \to H^* \to ZZ$	QCD Scale	$2\ell 2\nu$	14-18
$gg \to ZZ$	Parton Shower	4ℓ	38
$gg \to ZZ$	QCD Scale	$2\ell 2\nu$	18–20
$WZ+2j$	QCD Scale	$2\ell 2\nu$	20–22
$q\bar{q} \to ZZ+2j$	QCD Scale	4ℓ	8–14
$q\bar{q} \to ZZ+2j$	QCD Scale	$2\ell 2\nu$	8–16
$qq \to ZZ$ Control Regions			
$q\bar{q} \to ZZ$	QCD Scale	4ℓ	26
Three-lepton Control Regions			
$WZ+2j$	QCD Scale	$2\ell 2\nu$	28

servable bins but can reach up to 30% in some parts of the phase space.

In the 4ℓ channel, these uncertainties are parameterised using the 4ℓ invariant mass, transverse momentum, and the kinematics of the leading jets. NNs are trained to estimate the density ratio between the nominal and the varied samples in this multi-dimensional space [83]. This novel method ensures a detailed description of the systematic uncertainty while reducing statistical fluctuations due to the interpolation provided by the differentiable NN. In the 4ℓ channel, PS uncertainties are the leading source of uncertainties for the gluon–gluon processes in the SRs, and are about 30% and 40% in the yields of the signal and the background. The impact of PS uncertainties in the shape of observables is found to be no more than 10% in the 4ℓ channel. The PS uncertainties for the EW processes are less significant, ranging from a few percent to 10%. The PS uncertainties for the QCD $q\bar{q} \to ZZ$ background are generally smaller, at percentage level for most observable bins.

Experimental systematic uncertainties are generally less important than the theoretical ones. However, uncertainties related to jet reconstruction are important in the $2\ell 2\nu$ channel as mismeasurement of the jet energy can mimic $E_{\mathrm{T}}^{\mathrm{miss}}$. The main jet uncertainties are those in the jet energy scale (JES) and resolution (JER), which can amount to about 10% for processes in the EW SRs. The effect of pile-up and the differences between the energy responses for jets with different hadron flavour compositions are particularly important. Uncertainties originating from the electron and muon reconstruction and selection, and from $E_{\mathrm{T}}^{\mathrm{miss}}$ reconstruction are less important. The uncertainty in the Run-2 luminosity measurement is 1.7% [84], obtained using the LUCID-2 detector [85] for the primary luminosity measurements.

8. Results and interpretations

The statistical model used to translate the results into constraints on the off-shell signal strength $\mu_{\text{off-shell}}$ is based on the profile likelihood technique [86]. A binned likelihood function is constructed as a product of Poisson probability terms over all bins in all the SRs and CRs considered in the analysis, as introduced in Sections 5 and 6. The likelihood depends on the parameters of interest and a set of nuisance parameters $\boldsymbol{\theta}$ that include the effects of systematic uncertainties and statistical uncertainties from the limited number of simulated events. They are constrained using Gaussian and Poisson terms, respectively. Different parameters of interest are used depending on the interpretation. The first interpretation explores two signal strength parameters ($\mu_{\text{off-shell}}^{\text{ggF}} = \kappa_{g,\,\text{off-shell}}^2 \kappa_{V,\,\text{off-shell}}^2$ and $\mu_{\text{off-shell}}^{\text{EW}} = \kappa_{V,\,\text{off-shell}}^4$) corresponding to the ggF- and EW-induced off-shell contributions, respectively. Here, κ_g (κ_V) refers to the Higgs boson coupling to gluons (vector bosons) normalised to the SM prediction. In the second interpretation, a single off-shell signal-strength parameter ($\mu_{\text{off-shell}}$) is applied for all production modes, assuming that $\mu_{\text{off-shell}}^{\text{ggF}} = \mu_{\text{off-shell}}^{\text{EW}} = \mu_{\text{off-shell}}$.

Given the sizeable interference effects, the off-shell signal cannot be treated independently of the interfering backgrounds. The interference term, which is proportional to $\sqrt{\mu_{\text{off-shell}}}$, must be taken into account when building the probability model. The expected number of events from the $gg \to (H^* \to)ZZ$ process for a given $\mu_{\text{off-shell}}^{\text{ggF}}$, referred as ν^{ggF}, can be obtained for a bin of the input distributions from the following parameterisation:

$$
\begin{aligned}
&\nu^{\text{ggF}}(\mu_{\text{off-shell}}^{\text{ggF}}, \boldsymbol{\theta}) \\
&\quad = \mu_{\text{off-shell}}^{\text{ggF}} \cdot n_{\text{S}}^{\text{ggF}}(\boldsymbol{\theta}) \\
&\qquad + \sqrt{\mu_{\text{off-shell}}^{\text{ggF}}} \cdot (n_{\text{SBI}}^{\text{ggF}}(\boldsymbol{\theta}) - n_{\text{S}}^{\text{ggF}}(\boldsymbol{\theta}) - n_{\text{B}}^{\text{ggF}}(\boldsymbol{\theta})) + n_{\text{B}}^{\text{ggF}}(\boldsymbol{\theta}) \\
&\quad = (\mu_{\text{off-shell}}^{\text{ggF}} - \sqrt{\mu_{\text{off-shell}}^{\text{ggF}}}) \cdot n_{\text{S}}^{\text{ggF}}(\boldsymbol{\theta}) \\
&\qquad + \sqrt{\mu_{\text{off-shell}}^{\text{ggF}}} \cdot n_{\text{SBI}}^{\text{ggF}}(\boldsymbol{\theta}) + (1 - \sqrt{\mu_{\text{off-shell}}^{\text{ggF}}}) \cdot n_{\text{B}}^{\text{ggF}}(\boldsymbol{\theta})
\end{aligned}
$$

where $n_{\text{S}}^{\text{ggF}}$, $n_{\text{B}}^{\text{ggF}}$ and $n_{\text{SBI}}^{\text{ggF}}$ represent the corresponding expected yields of the signal, the $gg \to ZZ$ background and the full $gg \to (H^* \to)ZZ$ process, respectively. The expected number of events from the EW $q\bar{q} \to (H^* \to)ZZ + 2j$ process for a given $\mu_{\text{off-shell}}^{\text{EW}}$ can be modelled similarly, and the parameterisation is determined by using three simulation samples: that for the full process $q\bar{q} \to (H^* \to)ZZ + 2j$ with $\mu_{\text{off-shell}}^{\text{EW}}$ set to 1, that for the same process with $\mu_{\text{off-shell}}^{\text{EW}}$ set to 10, and the non-Higgs boson EW $q\bar{q} \to ZZ + 2j$ background[3]. The description in terms of a single signal component as performed for ggF production is not possible in the EW case because the requirement on high m_{ZZ}, used to ensure that the Higgs boson is off-shell, does not apply to the t-channel Higgs boson exchange in EW production, even though it is also off-shell (with t<0). The parameterisation described here ensures that this component scales with $\mu_{\text{off-shell}}^{\text{EW}}$.

The total normalisation of the $q\bar{q} \to ZZ$ background is left as a free parameter in the profile likelihood fit, separately for each jet multiplicity. Three parameters are introduced in the likelihood

---

[3] The values of $\mu_{\text{off-shell}}^{\text{EW}}$ = 0, 1, and 10 are chosen for technical reasons involving the production of simulated samples but in principle any three numbers could be used.

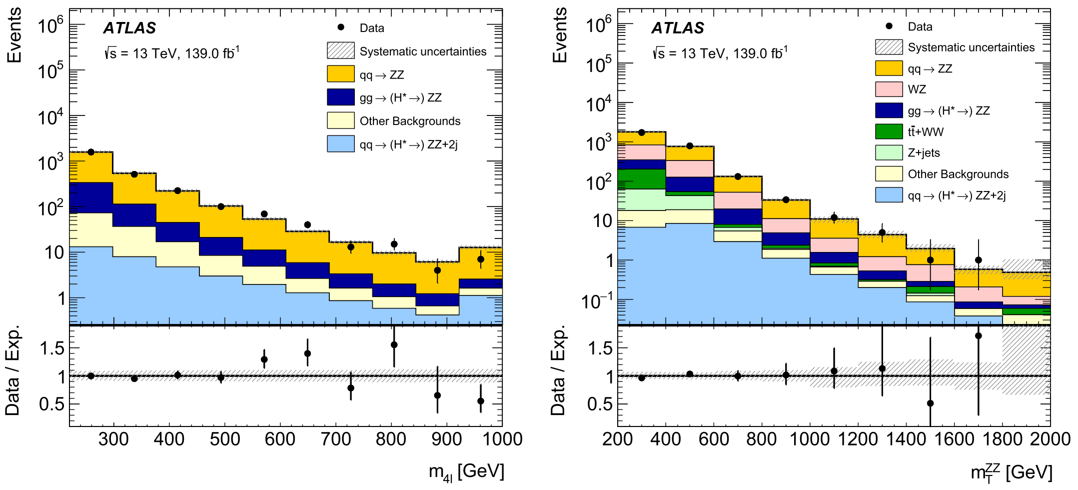

(a) (b)

Fig. 5. Comparisons between data and the SM prediction for the (a) $m_{4\ell}$ and (b) m_{T}^{ZZ} distributions in the inclusive off-shell signal regions in the $ZZ \to 4\ell$ and $ZZ \to 2\ell 2\nu$ channels, respectively. The scenario with the off-shell signal strength equal to one is considered in the fit. The hatched area represents the total systematic uncertainty. The last bin in both figures contains the overflow.

model to constrain the normalisation of this dominant background in both final states, a normalisation factor for 0-jet events, μ_{qqZZ}, and two additional parameters to represent the relative contributions of higher jet multiplicities, μ_{qqZZ}^{1j}, and μ_{qqZZ}^{2j}. The expected yield of 0-jet $q\bar{q} \to ZZ$ events is scaled by μ_{qqZZ}, that of 1-jet events by $\mu_{qqZZ} \cdot \mu_{qqZZ}^{1j}$, and that of events with at least two jets by $\mu_{qqZZ} \cdot \mu_{qqZZ}^{1j} \cdot \mu_{qqZZ}^{2j}$. These parameters are largely constrained by the three CRs defined in Section 5, especially at high jet multiplicity.

The normalisations of the WZ, Z + jets and non-resonant-$\ell\ell$ backgrounds are also obtained from the simultaneous fit, using the dedicated control regions described in Section 6. Similarly to the $q\bar{q} \to ZZ$ background, events from the WZ process are treated separately for each jet multiplicity. Five additional free parameters, $\mu_{3\ell}$, $\mu_{3\ell}^{1j}$, $\mu_{3\ell}^{2j}$, μ_{Zj}, and $\mu_{e\mu}$, are therefore introduced in the likelihood model specifically for the $2\ell 2\nu$ channel and for its combination with the 4ℓ channel.

The likelihood function for the combination of both channels is built as a product of the likelihoods of the individual channels. Theoretical and experimental uncertainties with common sources are treated as correlated between the two channels. The NLO EW uncertainty is uncorrelated between the two channels, due to the different schemes used to derive the uncertainties. The hypothesis of systematic uncertainty correlation between the 4ℓ and $2\ell 2\nu$ channels is tested for the dominant sources of uncertainties, including the PS uncertainties that use models with different complexity in the two channels, and the NLO EW uncertainty. The difference in the result when using different correlation hypotheses is found to be negligible.

The $m_{4\ell}$ distribution for the 4ℓ channel and the m_{T}^{ZZ} distribution for the $2\ell 2\nu$ channel are shown in Fig. 5 after the full fit to data with $\mu_{\text{off-shell}} = 1$. The total systematic uncertainty from the sources described in Section 7 are shown in the figure. The distributions of the NN observables used in the 4ℓ channel are shown in Fig. 3.

The expected numbers of events in the SRs after the maximum-likelihood fit to the data performed in all SRs and CRs, together with the corresponding observed yields, are shown in Tables 2 and 3 for the $ZZ \to 4\ell$ and $ZZ \to 2\ell 2\nu$ channels, respectively. The fitted background normalisation factors together with their total uncertainties are summarised in Table 4.

Table 2
The observed and expected yields together with their uncertainties, for the ggF- and EW-enriched categories in the 4ℓ channel. The results are obtained after the simultaneous fit to both the 4ℓ and $2\ell 2\nu$ channels with $\mu_{\text{off-shell}} = 1$. The first row represents the inclusive ZZ process from gg production, including the signal, background, and interference components. The signal and background components are shown separately in rows 2–3: they do not add up to match the inclusive yield due to the presence of negative interference. The other backgrounds include contributions from $t\bar{t}V$ and VVV processes. The uncertainties in the expected number of events include the statistical and systematic uncertainties. The uncertainties in the $qq \to ZZ$ background are quoted as the sum in quadrature of all three jet multiplicity contributions for purposes of illustration.

Process	ggF SR	Mixed SR	EW SR
$gg \to (H^* \to)ZZ$	341 + 117	42.5 + 14.9	11.8 + 4.3
$gg \to H^* \to ZZ$	32.6 + 9.07	3.68 + 1.03	1.58 + 0.47
$gg \to ZZ$	345 + 119	43.0 + 15.2	11.9 + 4.4
$q\bar{q} \to (H^* \to)ZZ + 2j$	23.2 + 1.0	2.03 + 0.16	9.89 + 0.96
$q\bar{q} \to ZZ$	1878 + 151	135 + 23	22.0 + 8.3
Other backgrounds	50.6 + 2.5	1.79 + 0.16	1.65 + 0.16
Total expected (SM)	2293 + 209	181 + 29	45.3 + 10.0
Observed	2327	178	50

To obtain the results for a given parameter of interest, profile likelihood ratios (denoted by λ) are computed for different values of each parameter. The $-2\ln\lambda$ curve as a function of $\mu_{\text{off-shell}}$ is presented in Fig. 6(a). The expected curve is constructed from a fit to an Asimov dataset which is built from the SM expectation. The expected curve is flatter than the observed due to the effect of a downward fluctuation in the data and the parabolic shape of the yield versus μ curve, which arises due to the $\sqrt{\mu}$ dependence of the interference. In particular, for electroweak production, the expected yield is minimised at the value of $\mu = 0.8$, close to the value $\mu = 1$ at which the expected $-2\ln\lambda$ curve is minimised. In this case, a downward fluctuation in the data, observed for this production mode, does not appreciably move the minimum, because a lower yield cannot reduce the best-fit value of μ below 0.8. Instead, the lower yield makes values further from the minimum less likely, thus narrowing the profile likelihood.

Due to the quadratic parameterisation of the yield as a function of the parameter of interest, the distribution of the test statistic $-2\ln\lambda$ is slightly different from the asymptotic χ^2 distribution predicted by Wilks' theorem [87]. Therefore confidence intervals on $\mu_{\text{off-shell}}$ are built based on the Neyman construction [88] using the distribution of $-2\ln\lambda$ for different values of the parameter of

Table 3
The observed and expected yields together with their uncertainties, for the ggF- and EW-enriched categories in the $2\ell 2\nu$ channel. The results are obtained after the simultaneous fit to both the 4ℓ and $2\ell 2\nu$ channels with $\mu_{\text{off-shell}} = 1$. The first row represents the inclusive ZZ process from gg production, including the signal, background, and interference components. The signal and background components are shown separately in rows 2–3: they do not add up to match the inclusive yield due to the presence of negative interference. The other backgrounds include contributions from VVV, W+jets and top quark processes other than pair production. The uncertainties in the expected number of events include the statistical and systematic uncertainties. The uncertainties in the $qq \to ZZ$ and WZ backgrounds are quoted as the sum in quadrature of all three jet multiplicity contributions for purposes of illustration.

Process	ggF SR	Mixed SR	EW SR
$gg \to (H^* \to)ZZ$	210 + 53	19.7 + 4.9	4.29 + 1.10
$gg \to H^* \to ZZ$	111 + 26	10.9 + 2.5	3.26 + 0.82
$gg \to ZZ$	251 + 66	23.4 + 6.2	5.31 + 1.46
$q\bar{q} \to (H^* \to)ZZ + 2j$	14.0 + 3.0	1.63 + 0.17	4.46 + 0.50
$q\bar{q} \to ZZ$	1422 + 112	80.4 + 11.9	7.74 + 2.99
WZ	678 + 54	51.9 + 6.9	7.89 + 2.50
Z+jets	62.3 + 24.3	7.51 + 6.94	0.62 + 0.54
Non-resonant-$\ell\ell$	106 + 39	9.17 + 2.73	1.55 + 0.42
Other backgrounds	22.6 + 5.2	1.62 + 0.25	1.40 + 0.10
Total expected (SM)	2515 + 165	172 + 17	28.0 + 4.1
Observed	2496	181	27

Table 4
The fitted normalisation factors for the dominant $q\bar{q} \to ZZ$ background as well as the WZ, Z+jets and non-resonant-$\ell\ell$ type backgrounds.

Normalisation factor	Fitted value
μ_{qqZZ}	1.11 ± 0.07
μ^{1j}_{qqZZ}	0.90 ± 0.10
μ^{2j}_{qqZZ}	0.88 ± 0.26
$\mu_{3\ell}$	1.06 ± 0.03
$\mu^{1j}_{3\ell}$	0.92 ± 0.10
$\mu^{2j}_{3\ell}$	0.75 ± 0.19
μ_{Zj}	0.90 ± 0.19
$\mu_{e\mu}$	1.08 ± 0.09

Table 5
The impact of most important systematic uncertainties on the observed upper value of $\mu_{\text{off-shell}}$ for which $-2\ln\lambda = 4$, obtained by the combined fit. This value corresponds to the two standard deviation upper limit of $\mu_{\text{off-shell}}$ with the asymptotic method. The first column denotes the systematic uncertainty that was excluded from the fit. The last row gives the nominal upper limit, where all uncertainties are included. The further the upper limit is deviating from the last row value, the more important that uncertainty is.

Systematic Uncertainty Fixed	$\mu_{\text{off-shell}}$ value at which $-2\ln\lambda(\mu_{\text{off-shell}}) = 4$
Parton shower uncertainty for $gg \to ZZ$ (normalisation)	2.26
Parton shower uncertainty for $gg \to ZZ$ (shape)	2.29
NLO EW uncertainty for $q\bar{q} \to ZZ$	2.27
NLO QCD uncertainty for $gg \to ZZ$	2.29
Parton shower uncertainty for $q\bar{q} \to ZZ$ (shape)	2.29
Jet energy scale and resolution uncertainty	2.26
None	2.30

interest. The distributions of $-2\ln\lambda$ are estimated using simulated events sampled from the likelihood model of the analysis, profiled to the best fit results from data. The resulting confidence intervals are 5–10% more conservative than those obtained by assuming that the asymptotic assumption is correct. The intersections of the 1-sigma and 2-sigma curves in Fig. 6(a) with the likelihood curves allow the true 68 and 95% confidence intervals to be estimated. The expected uncertainty in $\mu_{\text{off-shell}}$, also obtained using the 1σ confidence intervals from the Neyman construction, is ± 0.9. The observed value of $\mu_{\text{off-shell}}$ with the 1σ confidence intervals from the Neyman construction is $\mu_{\text{off-shell}} = 1.1^{+0.7}_{-0.6}$. The observed (expected) 95% confidence level (CL) upper limit on $\mu_{\text{off-shell}}$ is 2.4 (2.6). The background-only hypothesis ($\mu_{\text{off-shell}} = 0$) is rejected at an observed (expected) significance of 3.3σ (2.2σ). The $-2\ln\lambda = 2.30$ and $-2\ln\lambda = 5.99$ 2D contours for $\mu^{\text{ggF}}_{\text{off-shell}}$ and $\mu^{\text{EW}}_{\text{off-shell}}$, which correspond to the 68% and 95% CL limits in the asymptotic approximation, are shown in Fig. 6(b).

To estimate the importance of the most relevant sources of systematic uncertainty to the result, Table 5 shows the value of the largest $\mu_{\text{off-shell}}$ for which $-2\ln\lambda = 4$ when each source of uncertainty is removed one at a time. Due to the unusual shape of the yield curve, the impact of nuisance parameters on the best-fit value of $\mu_{\text{off-shell}}$ can be difficult to interpret. Additionally, the correlations between the nuisance parameters, and between the nuisance parameters and the normalisation parameters for the backgrounds, make it difficult to extract uncertainty components. Table 5 indicates the magnitude of the systematic uncertainties and shows their relative importance. The most important ones are the PS uncertainties, the NLO EW uncertainties, and the jet-related uncertainties.

The combination with the on-shell $H \to ZZ^* \to 4\ell$ analysis [89], where the on-shell signal strength is measured to be $\mu_{\text{on-shell}} = 1.01 \pm 0.11$, allows these results to be translated into limits on the width of the Higgs boson normalised to its SM expectation ($\mu_{\text{off-shell}}/\mu_{\text{on-shell}} = \Gamma_H/\Gamma_H^{\text{SM}}$) as well as the ratio of off-shell to on-shell couplings for ggF ($R_{gg} \equiv \kappa^2_{g,\text{ off-shell}}/\kappa^2_{g,\text{ on-shell}}$) and EW ($R_{VV} \equiv \kappa^2_{V,\text{ off-shell}}/\kappa^2_{V,\text{ on-shell}}$) production. The experimental uncertainties are correlated between the two measurements, while the theoretical uncertainties are assumed to be uncorrelated, considering that differences could exist in the structure of high-order corrections at different mass scales. The difference in the statistical results between the correlated and uncorrelated schemes is found to be negligible. The $\Gamma_H/\Gamma_H^{\text{SM}}$ interpretation assumes that the off- and on-shell coupling modifiers are the same for both ggF and EW production modes. The R_{gg} and R_{VV} interpretations assume that the total width of the Higgs boson is equal to its SM prediction, and that the scattering phase also follows the SM. Additionally, in the R_{gg} case it is assumed that the coupling scale factors associated with the on- and off-shell EW production are the same, while in the R_{VV} case the t-channel Higgs boson exchange process is assumed to scale in the same way as for the off-shell signal.

For the combination with the on-shell analysis, the combined likelihood is built as the product of the likelihood models for the two analyses. The values of $-2\ln\lambda$ as a function of $\Gamma_H/\Gamma_H^{\text{SM}}$, R_{gg} and R_{VV} are shown in Figs. 7(a), 7(b) and 7(c), respectively. The deviation of $-2\ln\lambda$ from a smooth parabolic curve in the region close to zero in Fig. 7(b) is due to the $\sqrt{\mu}$ dependence in the yield that arises from the interference, as discussed earlier in this section, combined with a slight excess observed in the data in the 4ℓ ggH SR, which leads to a maximum near $\mu = 0$. Confidence intervals are obtained using the Neyman construction, as described above. The corresponding measured values are the following: $\Gamma_H/\Gamma_H^{\text{SM}} = 1.1^{+0.7}_{-0.6}$, $R_{gg} = 1.4^{+1.1}_{-1.4}$ and $R_{VV} = 0.9^{+0.3}_{-0.3}$. Multiplying the measured $\Gamma_H/\Gamma_H^{\text{SM}}$ by the width of the SM Higgs boson, the measured Γ_H is $4.5^{+3.3}_{-2.5}$ MeV. The total uncertainty is dominated by its statistical component. The observed (expected) upper limit on $\Gamma_H/\Gamma_H^{\text{SM}}$ is 2.6 (2.7) at 95% confidence level using the Neyman construction, and the corresponding lower limit is 0.1 (0.01). Thus observed (expected) upper and lower limits can be placed on the total width of the Higgs boson of $0.5(0.1) < \Gamma_H < 10.5(10.9)$ MeV.

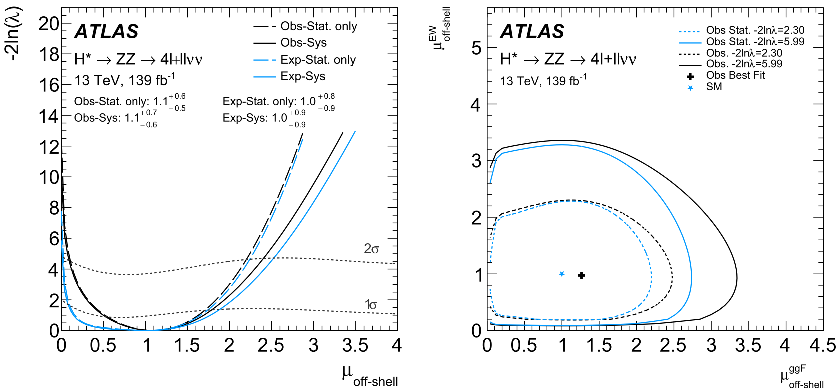

(a) (b)

Fig. 6. The likelihood profile, $-2\ln\lambda$, as a function of (a) the off-shell Higgs boson signal strength, $\mu_{\text{off-shell}}$, for the combination of the $ZZ \to 4\ell$ and $ZZ \to 2\ell 2\nu$ off-shell analyses, and (b) two off-shell signal strength parameters for the ggF and EW production modes, plotted in a plane ($\mu^{\text{ggF}}_{\text{off-shell}}$, $\mu^{\text{EW}}_{\text{off-shell}}$). In (a) the dotted curves correspond to the one and two standard deviation confidence intervals on the measurement obtained using the Newyman construction while (b) shows two-dimensional contours for $\mu^{\text{ggF}}_{\text{off-shell}}$ and $\mu^{\text{EW}}_{\text{off-shell}}$ corresponding to $-2\ln\lambda = 2.30$ and $-2\ln\lambda = 5.99$, which correspond to the 68% and 95% CL limits in the asymptotic approximation.

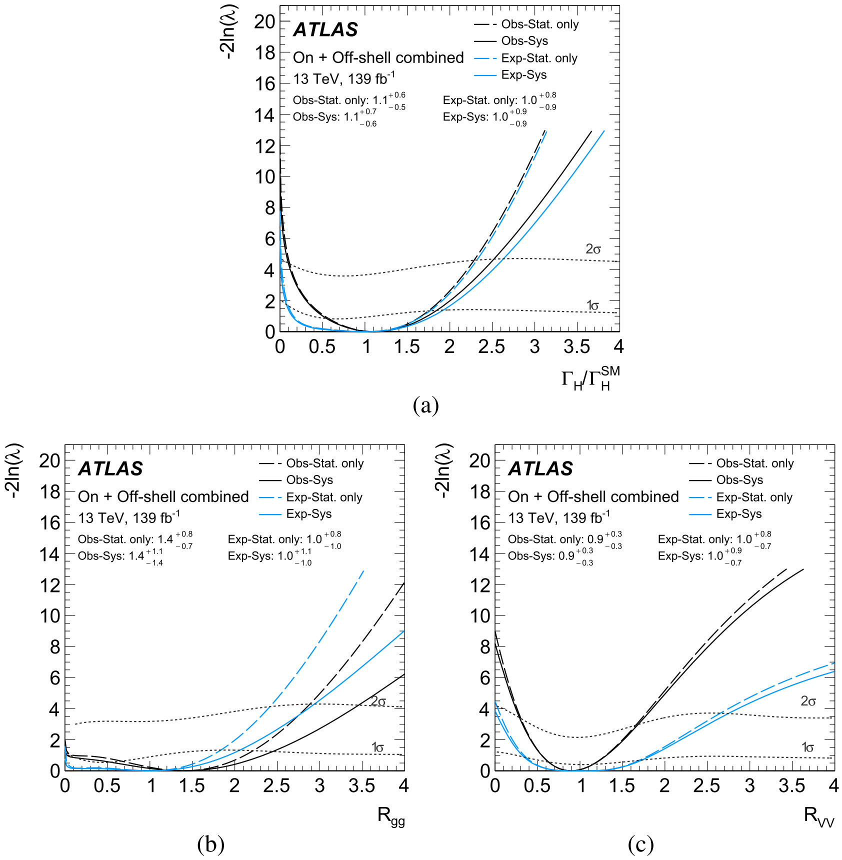

(a)

(b) (c)

Fig. 7. The likelihood profile, $-2\ln\lambda$, as a function of (a) $\Gamma_H/\Gamma_H^{\text{SM}}$, (b) R_{gg} and (c) R_{VV} for the combination with the on-shell signal strength measurement. The dotted curves correspond to the one and two standard deviation confidence intervals on the measurement obtained using the Neyman construction. For R_{gg} there are two additional negative crossings, near -1.2 and -0.84 from the best fit value: as these are very close to the 1-σ level, they are neglected.

9. Conclusion

This Letter presents a search for off-shell Higgs boson production in the $ZZ \to 4\ell$ and the $ZZ \to 2\ell 2\nu$ final states with the ATLAS detector using 139 fb^{-1} of pp collision data. The search is optimised for sensitivity to both the ggF- and EW-induced signal, and a simultaneous fit to all SRs and CRs is performed to extract the signal contribution. No deviations from the SM prediction are observed. The data reject the background-only hypothesis with an observed (expected) significance of 3.3σ (2.2σ). The observed (expected) upper limit at 95% confidence interval on the signal strength $\mu_{\text{off-shell}}$ is found to be 2.4 (2.6). A combination with the on-shell Higgs boson measurement gives a measured total width of the Higgs boson of $4.5^{+3.3}_{-2.5}$ MeV, and the observed (expected) upper limit on the total width is found to be 10.5 (10.9) MeV at 95% CL. These results are compatible with those previously obtained by the CMS experiment. Together with that result, this means that both experiments have observed evidence of off-shell Higgs boson production.

Declaration of competing interest

The authors declare that they have no known competing financial interests or personal relationships that could have appeared to influence the work reported in this paper.

Data availability

The data for this manuscript are not available. The values in the plots and tables associated to this article are stored in HEPDATA (https://hepdata.cedar.ac.uk).

Acknowledgements

We thank CERN for the very successful operation of the LHC, as well as the support staff from our institutions without whom ATLAS could not be operated efficiently.

We acknowledge the support of ANPCyT, Argentina; YerPhI, Armenia; ARC, Australia; BMWFW and FWF, Austria; ANAS, Azerbaijan; CNPq and FAPESP, Brazil; NSERC, NRC and CFI, Canada; CERN; ANID, Chile; CAS, MOST and NSFC, China; Minciencias, Colombia; MEYS CR, Czech Republic; DNRF and DNSRC, Denmark; IN2P3-CNRS and CEA-DRF/IRFU, France; SRNSFG, Georgia; BMBF, HGF and MPG, Germany; GSRI, Greece; RGC and Hong Kong SAR, China; ISF and Benoziyo Center, Israel; INFN, Italy; MEXT and JSPS, Japan; CNRST, Morocco; NWO, Netherlands; RCN, Norway; MEiN, Poland; FCT, Portugal; MNE/IFA, Romania; MESTD, Serbia; MSSR, Slovakia; ARRS and MIZŠ, Slovenia; DSI/NRF, South Africa; MICINN, Spain; SRC and Wallenberg Foundation, Sweden; SERI, SNSF and Canton of Bern and Geneva, Switzerland; MOST, Taiwan; TENMAK, Türkiye; STFC, United Kingdom; DOE and NSF, United States of America. In addition, individual groups and members have received support from BCKDF, CANARIE, Compute Canada and CRC, Canada; PRIMUS 21/SCI/017 and UNCE SCI/013, Czech Republic; COST, ERC, ERDF, Horizon 2020 and Marie Skłodowska-Curie Actions, European Union; Investissements d'Avenir Labex, Investissements d'Avenir Idex and ANR, France; DFG and AvH Foundation, Germany; Herakleitos, Thales and Aristeia programmes co-financed by EU-ESF and the Greek NSRF, Greece; BSF-NSF and MINERVA, Israel; Norwegian Financial Mechanism 2014-2021, Norway; NCN and NAWA, Poland; La Caixa Banking Foundation, CERCA Programme Generalitat de Catalunya and PROMETEO and GenT Programmes Generalitat Valenciana, Spain; Göran Gustafssons Stiftelse, Sweden; The Royal Society and Leverhulme Trust, United Kingdom.

The crucial computing support from all WLCG partners is acknowledged gratefully, in particular from CERN, the ATLAS Tier-1 facilities at TRIUMF (Canada), NDGF (Denmark, Norway, Sweden), CC-IN2P3 (France), KIT/GridKA (Germany), INFN-CNAF (Italy), NL-T1 (Netherlands), PIC (Spain), ASGC (Taiwan), RAL (UK) and BNL (USA), the Tier-2 facilities worldwide and large non-WLCG resource providers. Major contributors of computing resources are listed in Ref. [90].

References

[1] ATLAS Collaboration, Observation of a new particle in the search for the Standard Model Higgs boson with the ATLAS detector at the LHC, Phys. Lett. B 716 (2012) 1, arXiv:1207.7214 [hep-ex].
[2] CMS Collaboration, Observation of a new boson at a mass of 125 GeV with the CMS experiment at the LHC, Phys. Lett. B 716 (2012) 30, arXiv:1207.7235 [hep-ex].
[3] ATLAS Collaboration, A detailed map of Higgs boson interactions by the ATLAS experiment ten years after the discovery, Nature 607 (2022) 52, arXiv:2207.00092 [hep-ex].
[4] CMS Collaboration, A portrait of the Higgs boson by the CMS experiment ten years after the discovery, Nature 607 (2022) 60, arXiv:2207.00043 [hep-ex].
[5] LHC Higgs Cross Section Working Group, Handbook of LHC Higgs cross sections: 4. Deciphering the nature of the Higgs sector, arXiv:1610.07922 [hep-ph], 2016, 2/2017.
[6] N. Kauer, G. Passarino, Inadequacy of zero-width approximation for a light Higgs boson signal, J. High Energy Phys. 08 (2012) 116, arXiv:1206.4803 [hep-ph].
[7] F. Caola, K. Melnikov, Constraining the Higgs boson width with ZZ production at the LHC, Phys. Rev. D 88 (2013) 054024, arXiv:1307.4935 [hep-ph].
[8] J.M. Campbell, R.K. Ellis, C. Williams, Bounding the Higgs width at the LHC using full analytic results for gg $\to e^-e^+\mu^-\mu^+$, J. High Energy Phys. 04 (2014) 060, arXiv:1311.3589 [hep-ph].
[9] J.M. Campbell, R.K. Ellis, C. Williams, Bounding the Higgs width at the LHC: complementary results from $H \to WW$, Phys. Rev. D 89 (2014) 053011, arXiv:1312.1628 [hep-ph].
[10] C. Englert, M. Spannowsky, Limitations and opportunities of off-shell coupling measurements, Phys. Rev. D 90 (2014) 053003, arXiv:1405.0285 [hep-ph].
[11] G. Cacciapaglia, A. Deandrea, G.D. La Rochelle, J.-B. Flament, Higgs couplings: disentangling new physics with off-shell measurements, Phys. Rev. Lett. 113 (2014) 201802, arXiv:1406.1757 [hep-ph].
[12] A. Azatov, C. Grojean, A. Paul, E. Salvioni, Taming the off-shell Higgs boson, J. Exp. Theor. Phys. 120 (2015) 354, arXiv:1406.6338 [hep-ph].
[13] M. Ghezzi, G. Passarino, S. Uccirati, Bounding the Higgs width using effective field theory, PoS LL2014 072 (2014), arXiv:1405.1925 [hep-ph].
[14] M. Buschmann, et al., Mass effects in the Higgs-gluon coupling: boosted vs off-shell production, J. High Energy Phys. 02 (2015) 038, arXiv:1410.5806 [hep-ph].
[15] J.S. Gainer, J. Lykken, K.T. Matchev, S. Mrenna, M. Park, Beyond geolocating: constraining higher dimensional operators in $H \to 4\ell$ with off-shell production and more, Phys. Rev. D 91 (2015) 035011, arXiv:1403.4951 [hep-ph].
[16] C. Englert, Y. Soreq, M. Spannowsky, Off-shell Higgs coupling measurements in BSM scenarios, J. High Energy Phys. 05 (2015) 145, arXiv:1410.5440 [hep-ph].
[17] D. Goncalves, T. Han, S. Mukhopadhyay, Off-shell Higgs probe of naturalness, Phys. Rev. Lett. 120 (2018) 111801, arXiv:1710.02149 [hep-ph].
[18] D. Gonçalves, T. Han, S. Ching, Iris Leung, H. Qin, Off-shell Higgs couplings in $H^* \to ZZ \to \ell\ell\nu\nu$, Phys. Lett. B 817 (2021) 136329, arXiv:2012.05272 [hep-ph].
[19] S.J. Lee, M. Park, Z. Qian, Probing unitarity violation in the tail of the off-shell Higgs boson in V_LV_L mode, Phys. Rev. D 100 (2019) 011702, arXiv:1812.02679 [hep-ph].
[20] H.-R. He, X. Wan, Y.-K. Wang, Anomalous $H \to ZZ \to 4\ell$ decay and its interference effects on gluon–gluon contribution at the LHC, Chin. Phys. C 44 (2020) 123101, arXiv:1902.04756 [hep-ph].
[21] U. Haisch, G. Koole, Off-shell Higgs production at the LHC as a probe of the trilinear Higgs coupling, J. High Energy Phys. 02 (2022) 030, arXiv:2111.12589 [hep-ph].
[22] M. Ruhdorfer, E. Salvioni, A. Weiler, A global view of the off-shell Higgs portal, SciPost Phys. 8 (2020) 027, arXiv:1910.04170 [hep-ph].
[23] ATLAS Collaboration, Constraints on the off-shell Higgs boson signal strength in the high-mass ZZ and WW final states with the ATLAS detector, Eur. Phys. J. C 75 (2015) 335, arXiv:1503.01060 [hep-ex].
[24] CMS Collaboration, Constraints on the Higgs boson width from off-shell production and decay to Z-boson pairs, Phys. Lett. B 736 (2014) 64, arXiv:1405.3455 [hep-ex].
[25] CMS Collaboration, Limits on the Higgs boson lifetime and width from its decay to four charged leptons, Phys. Rev. D 92 (2015) 072010, arXiv:1507.06656.
[26] CMS Collaboration, Search for Higgs boson off-shell production in proton–proton collisions at 7 and 8 TeV and derivation of constraints on its total decay width, J. High Energy Phys. 09 (2016) 051, arXiv:1605.02329 [hep-ex].

[27] ATLAS Collaboration, Constraints on off-shell Higgs boson production and the Higgs boson total width in $ZZ \to 4\ell$ and $ZZ \to 2\ell 2\nu$ final states with the ATLAS detector, Phys. Lett. B 786 (2018) 223, arXiv:1808.01191 [hep-ex].

[28] CMS Collaboration, Measurements of the Higgs boson width and anomalous HVV couplings from on-shell and off-shell production in the four-lepton final state, Phys. Rev. D 99 (2019) 112003, arXiv:1901.00174 [hep-ex].

[29] CMS Collaboration, Measurement of the Higgs boson width and evidence of its off-shell contributions to ZZ production, Nat. Phys. 18 (2022) 1329, eprint: arXiv:2202.06923.

[30] S. Schael, et al., Precision electroweak measurements on the Z resonance, Phys. Rep. 427 (2006) 257, arXiv:hep-ex/0509008.

[31] ATLAS Collaboration, Measurements of the Higgs boson inclusive and differential fiducial cross sections in the 4ℓ decay channel at $\sqrt{s} = 13\,\text{TeV}$, Eur. Phys. J. C 80 (2020) 942, arXiv:2004.03969 [hep-ex].

[32] ATLAS Collaboration, The ATLAS experiment at the CERN large hadron collider, J. Instrum. 3 (2008) S08003.

[33] ATLAS Collaboration, ATLAS Insertable B-Layer Technical Design Report, CERN-LHCC-2010-013, ATLAS-TDR-19, https://cds.cern.ch/record/1291633, 2010, ATLAS Insertable B-Layer Technical Design Report Addendum, ATLAS-TDR-19-ADD-1 https://cds.cern.ch/record/1451888, 2012.

[34] ATLAS Collaboration, Performance of the ATLAS trigger system in 2015, Eur. Phys. J. C 77 (2017) 317, arXiv:1611.09661 [hep-ex].

[35] ATLAS Collaboration, The ATLAS Collaboration software and firmware, ATL-SOFT-PUB-2021-001, https://cds.cern.ch/record/2767187, 2021.

[36] ATLAS Collaboration, The ATLAS simulation infrastructure, Eur. Phys. J. C 70 (2010) 823, arXiv:1005.4568 [physics.ins-det].

[37] S. Agostinelli, et al., GEANT4: a simulation toolkit, Nucl. Instrum. Methods A 506 (2003) 250.

[38] T. Sjöstrand, S. Mrenna, P.Z. Skands, A brief introduction to PYTHIA 8.1, Comput. Phys. Commun. 178 (2008) 852, arXiv:0710.3820 [hep-ph].

[39] E. Bothmann, et al., Event generation with Sherpa 2.2, SciPost Phys. 7 (2019) 034, arXiv:1905.09127 [hep-ph].

[40] F. Buccioni, et al., OpenLoops 2, Eur. Phys. J. C 79 (2019) 866, arXiv:1907.13071 [hep-ph].

[41] F. Cascioli, P. Maieröfer, S. Pozzorini, Scattering amplitudes with open loops, Phys. Rev. Lett. 108 (2012) 111601, arXiv:1111.5206 [hep-ph].

[42] A. Denner, S. Dittmaier, L. Hofer, Collier: a fortran-based complex one-loop library in extended regularizations, Comput. Phys. Commun. 212 (2017) 220, arXiv:1604.06792 [hep-ph].

[43] R.D. Ball, et al., Parton distributions for the LHC Run II, J. High Energy Phys. 04 (2015) 040, arXiv:1410.8849 [hep-ph].

[44] F. Cascioli, et al., Precise Higgs-background predictions: merging NLO QCD and squared quark-loop corrections to four-lepton + 0, 1 jet production, J. High Energy Phys. 01 (2014) 046, arXiv:1309.0500 [hep-ph].

[45] F. Caola, K. Melnikov, R. Röntsch, L. Tancredi, QCD corrections to ZZ production in gluon fusion at the LHC, Phys. Rev. D 92 (2015) 18, arXiv:1509.06734 [hep-ph].

[46] F. Caola, M. Dowling, K. Melnikov, R. Röntsch, L. Tancredi, QCD corrections to vector boson pair production in gluon fusion including interference effects with off-shell Higgs at the LHC, J. High Energy Phys. 07 (2016) 087, arXiv:1605.04610 [hep-ph].

[47] G. Passarino, Higgs CAT, Eur. Phys. J. C 74 (2014) 2866, arXiv:1312.2397 [hep-ph].

[48] LHC Higgs Cross Section Working Group, D. de Florian, et al., Handbook of LHC Higgs Cross Sections: 4. Deciphering the Nature of the Higgs Sector, CERN-2017-002-M, CERN, Geneva, 2016, arXiv:1610.07922 [hep-ph].

[49] M. Bonvini, F. Caola, S. Forte, K. Melnikov, G. Ridolfi, Signal-background interference effects for gg $\to H \to W^+W^-$ beyond leading order, Phys. Rev. D 88 (3 2013) 034032, https://link.aps.org/doi/10.1103/PhysRevD.88.034032.

[50] F. Caola, K. Melnikov, R. Röntsch, L. Tancredi, QCD corrections to W+W - production through gluon fusion, Phys. Lett. B (ISSN 0370-2693) 754 (2016) 275.

[51] J. Alwall, et al., The automated computation of tree-level and next-to-leading order differential cross sections, and their matching to parton shower simulations, J. High Energy Phys. 07 (2014) 079, arXiv:1405.0301 [hep-ph].

[52] R.D. Ball, et al., Parton distributions with LHC data, Nucl. Phys. B 867 (2013) 244, arXiv:1207.1303 [hep-ph].

[53] ATLAS Collaboration, ATLAS Pythia 8 tunes to 7 TeV data, ATL-PHYS-PUB-2014-021, https://cds.cern.ch/record/1966419, 2014.

[54] S. Höche, F. Krauss, M. Schönherr, F. Siegert, QCD matrix elements + parton showers. The NLO case, J. High Energy Phys. 04 (2013) 027, arXiv:1207.5030 [hep-ph].

[55] B. Biedermann, A. Denner, S. Dittmaier, L. Hofer, B. Jäger, Electroweak corrections to $pp \to \mu^+\mu^-e^+e^- + X$ at the LHC: a Higgs boson background study, Phys. Rev. Lett. 116 (2016) 161803, arXiv:1601.07787 [hep-ph].

[56] B. Biedermann, A. Denner, S. Dittmaier, L. Hofer, B. Jäger, Next-to-leading-order electroweak corrections to the production of four charged leptons at the LHC, J. High Energy Phys. 01 (2017) 033, arXiv:1611.05338 [hep-ph].

[57] S. Kallweit, J. Lindert, S. Pozzorini, M. Schönherr, NLO QCD+EW predictions for $2\ell 2\nu$ diboson signatures at the LHC, J. High Energy Phys. 11 (2017) 120, arXiv:1705.00598 [hep-ph].

[58] P. Nason, G. Zanderighi, W^+W^-, WZ and ZZ production in the POWHEG-BOX-V2, Eur. Phys. J. C 74 (2014) 2702, arXiv:1311.1365 [hep-ph].

[59] R. Gavin, Y. Li, F. Petriello, S. Quackenbush, FEWZ 2.0: a code for hadronic Z production at next-to-next-to-leading order, Comput. Phys. Commun. 182 (2011) 2388, arXiv:1011.3540 [hep-ph].

[60] M. Czakon, A. Mitov, Top++: a program for the calculation of the top-pair cross-section at hadron colliders, Comput. Phys. Commun. 185 (2014) 2930, arXiv:1112.5675 [hep-ph].

[61] P. Kant, et al., HatHor for single top-quark production: updated predictions and uncertainty estimates for single top-quark production in hadronic collisions, Comput. Phys. Commun. 191 (2015) 74, arXiv:1406.4403 [hep-ph].

[62] M. Aliev, et al., HATHOR: HAdronic top and heavy quarks crOss section calculatoR, Comput. Phys. Commun. 182 (2011) 1034, arXiv:1007.1327 [hep-ph].

[63] S. Frixione, V. Hirschi, D. Pagani, H.-S. Shao, M. Zaro, Electroweak and QCD corrections to top-pair hadroproduction in association with heavy bosons, J. High Energy Phys. 06 (2015) 184, arXiv:1504.03446 [hep-ph].

[64] ATLAS Collaboration, Search for heavy resonances decaying into a pair of Z bosons in the $\ell^+\ell^-\ell'^+\ell'^-$ and $\ell^+\ell^-\nu\bar{\nu}$ final states using $139\,\text{fb}^{-1}$ of proton–proton collisions at $\sqrt{s} = 13\,\text{TeV}$ with the ATLAS detector, Eur. Phys. J. C 81 (2020) 332, arXiv:2009.14791 [hep-ex].

[65] ATLAS Collaboration, Muon reconstruction performance of the ATLAS detector in proton–proton collision data at $\sqrt{s} = 13\,\text{TeV}$, Eur. Phys. J. C 76 (2016) 292, arXiv:1603.05598 [hep-ex].

[66] ATLAS Collaboration, Electron reconstruction and identification in the ATLAS experiment using the 2015 and 2016 LHC proton–proton collision data at $\sqrt{s} = 13\,\text{TeV}$, Eur. Phys. J. C 79 (2019) 639, arXiv:1902.04655 [hep-ex].

[67] ATLAS Collaboration, Jet reconstruction and performance using particle flow with the ATLAS detector, Eur. Phys. J. C 77 (2017) 466, arXiv:1703.10485 [hep-ex].

[68] M. Cacciari, G.P. Salam, G. Soyez, The anti-k_t jet clustering algorithm, J. High Energy Phys. 04 (2008) 063, arXiv:0802.1189 [hep-ph].

[69] M. Cacciari, G.P. Salam, G. Soyez, FastJet user manual, Eur. Phys. J. C 72 (2012) 1896, arXiv:1111.6097 [hep-ph].

[70] ATLAS Collaboration, Jet energy scale measurements and their systematic uncertainties in proton-proton collisions at $\sqrt{s} = 13$ TeV with the ATLAS detector, Phys. Rev. D 96 (2017) 072002, arXiv:1703.09665 [hep-ex].

[71] ATLAS Collaboration, Performance of pile-up mitigation techniques for jets in pp collisions at $\sqrt{s} = 8\,\text{TeV}$ using the ATLAS detector, Eur. Phys. J. C 76 (2016) 581, arXiv:1510.03823 [hep-ex].

[72] ATLAS Collaboration, Identification and rejection of pile-up jets at high pseudorapidity with the ATLAS detector, Eur. Phys. J. C 77 (2017) 580, Erratum: Eur. Phys. J. C 77 (2017) 712, arXiv:1705.02211 [hep-ex].

[73] ATLAS Collaboration, ATLAS b-jet identification performance and efficiency measurement with $t\bar{t}$ events in pp collisions at $\sqrt{s} = 13$ TeV, Eur. Phys. J. C 79 (2019) 970, arXiv:1907.05120 [hep-ex].

[74] ATLAS flavour-tagging algorithms for the LHC Run 2 pp collision dataset, arXiv:2211.16345 [physics.data-an], 2022.

[75] ATLAS Collaboration, Performance of missing transverse momentum reconstruction with the ATLAS detector in the first proton–proton collisions at $\sqrt{s} = 13\ TeV$, ATL-PHYS-PUB-2015-027, https://cds.cern.ch/record/2037904, 2015.

[76] ATLAS Collaboration, Object-based missing transverse momentum significance in the ATLAS detector, ATLAS-CONF-2018-038, https://cds.cern.ch/record/2630948, 2018.

[77] F. Chollet, et al., https://github.com/fchollet/keras, 2015.

[78] Martín Abadi, et al., TensorFlow: large-scale machine learning on heterogeneous systems, Software available from tensorflow.org, https://www.tensorflow.org/, 2015.

[79] ATLAS Collaboration, Evidence for the spin-0 nature of the Higgs boson using ATLAS data, Phys. Lett. B 726 (2013) 120, arXiv:1307.1432 [hep-ex].

[80] D. Rainwater, R. Szalapski, D. Zeppenfeld, Probing color-singlet exchange in $Z+$ 2-jet events at the CERN LHC, Phys. Rev. D 54 (11 1996) 6680, https://link.aps.org/doi/10.1103/PhysRevD.54.6680.

[81] D. de Florian, et al., Handbook of LHC Higgs cross sections: 4. Deciphering the nature of the Higgs sector, arXiv:1610.07922 [hep-ph], 2016.

[82] S. Gieseke, T. Kasprzik, J.H. Kühn, Vector-boson pair production and electroweak corrections in HERWIG++, Eur. Phys. J. C 74 (2014) 2988, arXiv:1401.3964 [hep-ph].

[83] B. Nachman, J. Thaler, Neural conditional reweighting, Phys. Rev. D 105 (2022) 076015, arXiv:2107.08979 [physics.data-an].

[84] ATLAS Collaboration, Luminosity determination in pp collisions at $\sqrt{s} = 13\,\text{TeV}$ using the ATLAS detector at the LHC, ATLAS-CONF-2019-021, https://cds.cern.ch/record/2677054, 2019.

[85] G. Avoni, et al., The new LUCID-2 detector for luminosity measurement and monitoring in ATLAS, J. Instrum. 13 (2018) P07017.

[86] G. Cowan, K. Cranmer, E. Gross, O. Vitells, Asymptotic formulae for likelihood-based tests of new physics, Eur. Phys. J. C 71 (2011).

[87] S.S. Wilks, The large-sample distribution of the likelihood ratio for testing composite hypotheses, Ann. Math. Stat. 9 (1938) 60.

[88] J. Neyman, Outline of a theory of statistical estimation based on the classical theory of probability, Philos. Trans. R. Soc. Lond. Ser. A, Math. Phys. Sci. 236 (1937) 333, issn: 00804614.

[89] ATLAS Collaboration, Higgs boson production cross-section measurements and their EFT interpretation in the 4ℓ decay channel at $\sqrt{s} = 13\,TeV$ with the ATLAS detector, Eur. Phys. J. C 80 (2020) 957, arXiv:2004.03447 [hep-ex], Erratum: Eur. Phys. J. C 81 (2021) 29, Erratum: Eur. Phys. J. C 81 (2021) 398.

[90] ATLAS Collaboration, ATLAS computing acknowledgements, ATL-SOFT-PUB-2023-001, https://cds.cern.ch/record/2869272, 2023.

The ATLAS Collaboration

G. Aad[102], B. Abbott[120], K. Abeling[55], S.H. Abidi[29], A. Aboulhorma[35e], H. Abramowicz[151], H. Abreu[150], Y. Abulaiti[117], A.C. Abusleme Hoffman[137a], B.S. Acharya[69a,69b,p], C. Adam Bourdarios[4], L. Adamczyk[85a], L. Adamek[155], S.V. Addepalli[26], J. Adelman[115], A. Adiguzel[21c], S. Adorni[56], T. Adye[134], A.A. Affolder[136], Y. Afik[36], M.N. Agaras[13], J. Agarwala[73a,73b], A. Aggarwal[100], C. Agheorghiesei[27c], J.A. Aguilar-Saavedra[130f], A. Ahmad[36], F. Ahmadov[38,ab], W.S. Ahmed[104], S. Ahuja[95], X. Ai[48], G. Aielli[76a,76b], M. Ait Tamlihat[35e], B. Aitbenchikh[35a], I. Aizenberg[169], M. Akbiyik[100], T.P.A. Åkesson[98], A.V. Akimov[37], N.N. Akolkar[24], K. Al Khoury[41], G.L. Alberghi[23b], J. Albert[165], P. Albicocco[53], S. Alderweireldt[52], M. Aleksa[36], I.N. Aleksandrov[38], C. Alexa[27b], T. Alexopoulos[10], A. Alfonsi[114], F. Alfonsi[23b], M. Alhroob[120], B. Ali[132], S. Ali[148], M. Aliev[37], G. Alimonti[71a], W. Alkakhi[55], C. Allaire[66], B.M.M. Allbrooke[146], C.A. Allendes Flores[137f], P.P. Allport[20], A. Aloisio[72a,72b], F. Alonso[90], C. Alpigiani[138], M. Alvarez Estevez[99], A. Alvarez Fernandez[100], M.G. Alviggi[72a,72b], M. Aly[101], Y. Amaral Coutinho[82b], A. Ambler[104], C. Amelung[36], M. Amerl[101], C.G. Ames[109], D. Amidei[106], S.P. Amor Dos Santos[130a], K.R. Amos[163], V. Ananiev[125], C. Anastopoulos[139], T. Andeen[11], J.K. Anders[36], S.Y. Andrean[47a,47b], A. Andreazza[71a,71b], S. Angelidakis[9], A. Angerami[41,ae], A.V. Anisenkov[37], A. Annovi[74a], C. Antel[56], M.T. Anthony[139], E. Antipov[145], M. Antonelli[53], D.J.A. Antrim[17a], F. Anulli[75a], M. Aoki[83], T. Aoki[153], J.A. Aparisi Pozo[163], M.A. Aparo[146], L. Aperio Bella[48], C. Appelt[18], N. Aranzabal[36], V. Araujo Ferraz[82a], C. Arcangeletti[53], A.T.H. Arce[51], E. Arena[92], J-F. Arguin[108], S. Argyropoulos[54], J.-H. Arling[48], A.J. Armbruster[36], O. Arnaez[4], H. Arnold[114], Z.P. Arrubarrena Tame[109], G. Artoni[75a,75b], H. Asada[111], K. Asai[118], S. Asai[153], N.A. Asbah[61], J. Assahsah[35d], K. Assamagan[29], R. Astalos[28a], R.J. Atkin[33a], M. Atkinson[162], N.B. Atlay[18], H. Atmani[62b], P.A. Atmasiddha[106], K. Augsten[132], S. Auricchio[72a,72b], A.D. Auriol[20], V.A. Austrup[171], G. Avner[150], G. Avolio[36], K. Axiotis[56], G. Azuelos[108,ai], D. Babal[28b], H. Bachacou[135], K. Bachas[152,s], A. Bachiu[34], F. Backman[47a,47b], A. Badea[61], P. Bagnaia[75a,75b], M. Bahmani[18], A.J. Bailey[163], V.R. Bailey[162], J.T. Baines[134], C. Bakalis[10], O.K. Baker[172], E. Bakos[15], D. Bakshi Gupta[8], R. Balasubramanian[114], E.M. Baldin[37], P. Balek[133], E. Ballabene[71a,71b], F. Balli[135], L.M. Baltes[63a], W.K. Balunas[32], J. Balz[100], E. Banas[86], M. Bandieramonte[129], A. Bandyopadhyay[24], S. Bansal[24], L. Barak[151], E.L. Barberio[105], D. Barberis[57b,57a], M. Barbero[102], G. Barbour[96], K.N. Barends[33a], T. Barillari[110], M-S. Barisits[36], T. Barklow[143], P. Baron[122], D.A. Baron Moreno[101], A. Baroncelli[62a], G. Barone[29], A.J. Barr[126], L. Barranco Navarro[47a,47b], F. Barreiro[99], J. Barreiro Guimarães da Costa[14a], U. Barron[151], M.G. Barros Teixeira[130a], S. Barsov[37], F. Bartels[63a], R. Bartoldus[143], A.E. Barton[91], P. Bartos[28a], A. Basan[100], M. Baselga[49], I. Bashta[77a,77b], A. Bassalat[66,b], M.J. Basso[155], C.R. Basson[101], R.L. Bates[59], S. Batlamous[35e], J.R. Batley[32], B. Batool[141], M. Battaglia[136], D. Battulga[18], M. Bauce[75a,75b], M. Bauer[36], P. Bauer[24], J.B. Beacham[51], T. Beau[127], P.H. Beauchemin[158], F. Becherer[54], P. Bechtle[24], H.P. Beck[19,r], K. Becker[167], A.J. Beddall[21d], V.A. Bednyakov[38], C.P. Bee[145], L.J. Beemster[15], T.A. Beermann[36], M. Begalli[82d], M. Begel[29], A. Behera[145], J.K. Behr[48], C. Beirao Da Cruz E Silva[36], J.F. Beirer[55,36], F. Beisiegel[24], M. Belfkir[159], G. Bella[151], L. Bellagamba[23b], A. Bellerive[34], P. Bellos[20], K. Beloborodov[37], N.L. Belyaev[37], D. Benchekroun[35a], F. Bendebba[35a], Y. Benhammou[151], M. Benoit[29], J.R. Bensinger[26], S. Bentvelsen[114], L. Beresford[48], M. Beretta[53], E. Bergeaas Kuutmann[161], N. Berger[4], B. Bergmann[132], J. Beringer[17a], S. Berlendis[7], G. Bernardi[5], C. Bernius[143], F.U. Bernlochner[24], T. Berry[95], P. Berta[133], A. Berthold[50], I.A. Bertram[91], S. Bethke[110], A. Betti[75a,75b], A.J. Bevan[94], M. Bhamjee[33c], S. Bhatta[145], D.S. Bhattacharya[166], P. Bhattarai[26], V.S. Bhopatkar[121], R. Bi[29,ak], R.M. Bianchi[129], O. Biebel[109], R. Bielski[123], M. Biglietti[77a], T.R.V. Billoud[132], M. Bindi[55], A. Bingul[21b], C. Bini[75a,75b], A. Biondini[92], C.J. Birch-sykes[101], G.A. Bird[20,134], M. Birman[169], M. Biros[133], T. Bisanz[36], E. Bisceglie[43b,43a], D. Biswas[170], A. Bitadze[101], K. Bjørke[125], I. Bloch[48], C. Blocker[26], A. Blue[59], U. Blumenschein[94], J. Blumenthal[100], G.J. Bobbink[114], V.S. Bobrovnikov[37], M. Boehler[54], D. Bogavac[36], A.G. Bogdanchikov[37], C. Bohm[47a], V. Boisvert[95], P. Bokan[48], T. Bold[85a], M. Bomben[5], M. Bona[94], M. Boonekamp[135], C.D. Booth[95], A.G. Borbély[59], H.M. Borecka-Bielska[108], L.S. Borgna[96], G. Borissov[91], D. Bortoletto[126], D. Boscherini[23b], M. Bosman[13], J.D. Bossio Sola[36], K. Bouaouda[35a], N. Bouchhar[163], J. Boudreau[129], E.V. Bouhova-Thacker[91], D. Boumediene[40], R. Bouquet[5], A. Boveia[119], J. Boyd[36], D. Boye[29], I.R. Boyko[38], J. Bracinik[20], N. Brahimi[62d], G. Brandt[171], O. Brandt[32], F. Braren[48], B. Brau[103], J.E. Brau[123], K. Brendlinger[48], R. Brener[169], L. Brenner[114], R. Brenner[161], S. Bressler[169], D. Britton[59], D. Britzger[110], I. Brock[24], G. Brooijmans[41], W.K. Brooks[137f], E. Brost[29], L.M. Brown[165], T.L. Bruckler[126], P.A. Bruckman de Renstrom[86], B. Brüers[48], D. Bruncko[28b,*], A. Bruni[23b], G. Bruni[23b], M. Bruschi[23b], N. Bruscino[75a,75b], T. Buanes[16], Q. Buat[138], A.G. Buckley[59], I.A. Budagov[38,*], M.K. Bugge[125], O. Bulekov[37], B.A. Bullard[143], S. Burdin[92], C.D. Burgard[49], A.M. Burger[40], B. Burghgrave[8], O. Burlayenko[54], J.T.P. Burr[32], C.D. Burton[11], J.C. Burzynski[142], E.L. Busch[41], V. Büscher[100], P.J. Bussey[59], J.M. Butler[25], C.M. Buttar[59], J.M. Butterworth[96], W. Buttinger[134], C.J. Buxo Vazquez[107], A.R. Buzykaev[37], G. Cabras[23b], S. Cabrera Urbán[163], D. Caforio[58], H. Cai[129], Y. Cai[14a,14e], V.M.M. Cairo[36], O. Cakir[3a], N. Calace[36], P. Calafiura[17a], G. Calderini[127], P. Calfayan[68], G. Callea[59], L.P. Caloba[82b], D. Calvet[40], S. Calvet[40], T.P. Calvet[102], M. Calvetti[74a,74b], R. Camacho Toro[127], S. Camarda[36], D. Camarero Munoz[26], P. Camarri[76a,76b], M.T. Camerlingo[72a,72b], D. Cameron[125], C. Camincher[165], M. Campanelli[96], A. Camplani[42], V. Canale[72a,72b], A. Canesse[104], M. Cano Bret[80], J. Cantero[163], Y. Cao[162], F. Capocasa[26], M. Capua[43b,43a], A. Carbone[71a,71b], R. Cardarelli[76a], J.C.J. Cardenas[8], F. Cardillo[163], T. Carli[36], G. Carlino[72a], J.I. Carlotto[13], B.T. Carlson[129,t], E.M. Carlson[165,156a], L. Carminati[71a,71b], M. Carnesale[75a,75b], S. Caron[113], E. Carquin[137f], S. Carrá[71a,71b], G. Carratta[23b,23a], F. Carrio Argos[33g], J.W.S. Carter[155], T.M. Carter[52], M.P. Casado[13,j], A.F. Casha[155], M. Caspar[48], E.G. Castiglia[172], F.L. Castillo[63a], L. Castillo Garcia[13], V. Castillo Gimenez[163], N.F. Castro[130a,130e], A. Catinaccio[36], J.R. Catmore[125], V. Cavaliere[29], N. Cavalli[23b,23a], V. Cavasinni[74a,74b], E. Celebi[21a], F. Celli[126], M.S. Centonze[70a,70b], K. Cerny[122], A.S. Cerqueira[82a], A. Cerri[146],

L. Cerrito[76a,76b], F. Cerutti[17a], A. Cervelli[23b], G. Cesarini[53], S.A. Cetin[21d], Z. Chadi[35a],
D. Chakraborty[115], M. Chala[130f], J. Chan[170], W.Y. Chan[153], J.D. Chapman[32],
B. Chargeishvili[149b], D.G. Charlton[20], T.P. Charman[94], M. Chatterjee[19], C. Chauhan[133],
S. Chekanov[6], S.V. Chekulaev[156a], G.A. Chelkov[38,a], A. Chen[106], B. Chen[151], B. Chen[165],
H. Chen[14c], H. Chen[29], J. Chen[62c], J. Chen[142], S. Chen[153], S.J. Chen[14c], X. Chen[62c],
X. Chen[14b,ah], Y. Chen[62a], C.L. Cheng[170], H.C. Cheng[64a], S. Cheong[143], A. Cheplakov[38],
E. Cheremushkina[48], E. Cherepanova[114], R. Cherkaoui El Moursli[35e], E. Cheu[7], K. Cheung[65],
L. Chevalier[135], V. Chiarella[53], G. Chiarelli[74a], N. Chiedde[102], G. Chiodini[70a],
A.S. Chisholm[20], A. Chitan[27b], M. Chitishvili[163], M.V. Chizhov[38], K. Choi[11],
A.R. Chomont[75a,75b], Y. Chou[103], E.Y.S. Chow[114], T. Chowdhury[33g], L.D. Christopher[33g],
K.L. Chu[64a], M.C. Chu[64a], X. Chu[14a,14e], J. Chudoba[131], J.J. Chwastowski[86], D. Cieri[110],
K.M. Ciesla[85a], V. Cindro[93], A. Ciocio[17a], F. Cirotto[72a,72b], Z.H. Citron[169,m], M. Citterio[71a],
D.A. Ciubotaru[27b], B.M. Ciungu[155], A. Clark[56], P.J. Clark[52], J.M. Clavijo Columbie[48],
S.E. Clawson[101], C. Clement[47a,47b], J. Clercx[48], L. Clissa[23b,23a], Y. Coadou[102],
M. Cobal[69a,69c], A. Coccaro[57b], R.F. Coelho Barrue[130a], R. Coelho Lopes De Sa[103],
S. Coelli[71a], H. Cohen[151], A.E.C. Coimbra[71a,71b], B. Cole[41], J. Collot[60],
P. Conde Muiño[130a,130g], M.P. Connell[33c], S.H. Connell[33c], I.A. Connelly[59], E.I. Conroy[126],
F. Conventi[72a,aj], H.G. Cooke[20], A.M. Cooper-Sarkar[126], F. Cormier[164], L.D. Corpe[36],
M. Corradi[75a,75b], F. Corriveau[104,z], A. Cortes-Gonzalez[18], M.J. Costa[163], F. Costanza[4],
D. Costanzo[139], B.M. Cote[119], G. Cowan[95], K. Cranmer[117], S. Crépé-Renaudin[60],
F. Crescioli[127], M. Cristinziani[141], M. Cristoforetti[78a,78b,d], V. Croft[114], G. Crosetti[43b,43a],
A. Cueto[36], T. Cuhadar Donszelmann[160], H. Cui[14a,14e], Z. Cui[7], W.R. Cunningham[59],
F. Curcio[43b,43a], P. Czodrowski[36], M.M. Czurylo[63b], M.J. Da Cunha Sargedas De Sousa[62a],
J.V. Da Fonseca Pinto[82b], C. Da Via[101], W. Dabrowski[85a], T. Dado[49], S. Dahbi[33g], T. Dai[106],
C. Dallapiccola[103], M. Dam[42], G. D'amen[29], V. D'Amico[109], J. Damp[100], J.R. Dandoy[128],
M.F. Daneri[30], M. Danninger[142], V. Dao[36], G. Darbo[57b], S. Darmora[6], S.J. Das[29,ak],
S. D'Auria[71a,71b], C. David[156b], T. Davidek[133], B. Davis-Purcell[34], I. Dawson[94], K. De[8],
R. De Asmundis[72a], N. De Biase[48], S. De Castro[23b,23a], N. De Groot[113], P. de Jong[114],
H. De la Torre[107], A. De Maria[14c], A. De Salvo[75a], U. De Sanctis[76a,76b], A. De Santo[146],
J.B. De Vivie De Regie[60], D.V. Dedovich[38], J. Degens[114], A.M. Deiana[44], F. Del Corso[23b,23a],
J. Del Peso[99], F. Del Rio[63a], F. Deliot[135], C.M. Delitzsch[49], M. Della Pietra[72a,72b],
D. Della Volpe[56], A. Dell'Acqua[36], L. Dell'Asta[71a,71b], M. Delmastro[4], P.A. Delsart[60],
S. Demers[172], M. Demichev[38], S.P. Denisov[37], L. D'Eramo[115], D. Derendarz[86], F. Derue[127],
P. Dervan[92], K. Desch[24], K. Dette[155], C. Deutsch[24], F.A. Di Bello[57b,57a],
A. Di Ciaccio[76a,76b], L. Di Ciaccio[4], A. Di Domenico[75a,75b], C. Di Donato[72a,72b],
A. Di Girolamo[36], G. Di Gregorio[5], A. Di Luca[78a,78b], B. Di Micco[77a,77b], R. Di Nardo[77a,77b],
C. Diaconu[102], F.A. Dias[114], T. Dias Do Vale[142], M.A. Diaz[137a,137b], F.G. Diaz Capriles[24],
M. Didenko[163], E.B. Diehl[106], L. Diehl[54], S. Díez Cornell[48], C. Diez Pardos[141],
C. Dimitriadi[24,161], A. Dimitrievska[17a], J. Dingfelder[24], I-M. Dinu[27b], S.J. Dittmeier[63b],
F. Dittus[36], F. Djama[102], T. Djobava[149b], J.I. Djuvsland[16], C. Doglioni[101,98], J. Dolejsi[133],
Z. Dolezal[133], M. Donadelli[82c], B. Dong[107], J. Donini[40], A. D'Onofrio[77a,77b],
M. D'Onofrio[92], J. Dopke[134], A. Doria[72a], M.T. Dova[90], A.T. Doyle[59], M.A. Draguet[126],

E. Drechsler[142], E. Dreyer[169], I. Drivas-koulouris[10], A.S. Drobac[158], M. Drozdova[56], D. Du[62a], T.A. du Pree[114], F. Dubinin[37], M. Dubovsky[28a], E. Duchovni[169], G. Duckeck[109], O.A. Ducu[27b], D. Duda[110], A. Dudarev[36], E.R. Duden[26], M. D'uffizi[101], L. Duflot[66], M. Dührssen[36], C. Dülsen[171], A.E. Dumitriu[27b], M. Dunford[63a], S. Dungs[49], K. Dunne[47a,47b], A. Duperrin[102], H. Duran Yildiz[3a], M. Düren[58], A. Durglishvili[149b], B.L. Dwyer[115], G.I. Dyckes[17a], M. Dyndal[85a], S. Dysch[101], B.S. Dziedzic[86], Z.O. Earnshaw[146], B. Eckerova[28a], S. Eggebrecht[55], M.G. Eggleston[51], E. Egidio Purcino De Souza[127], L.F. Ehrke[56], G. Eigen[16], K. Einsweiler[17a], T. Ekelof[161], P.A. Ekman[98], Y. El Ghazali[35b], H. El Jarrari[35e,148], A. El Moussaouy[35a], V. Ellajosyula[161], M. Ellert[161], F. Ellinghaus[171], A.A. Elliot[94], N. Ellis[36], J. Elmsheuser[29], M. Elsing[36], D. Emeliyanov[134], Y. Enari[153], I. Ene[17a], S. Epari[13], J. Erdmann[49], P.A. Erland[86], M. Errenst[171], M. Escalier[66], C. Escobar[163], E. Etzion[151], G. Evans[130a], H. Evans[68], L.S. Evans[95], M.O. Evans[146], A. Ezhilov[37], S. Ezzarqtouni[35a], F. Fabbri[59], L. Fabbri[23b,23a], G. Facini[96], V. Fadeyev[136], R.M. Fakhrutdinov[37], S. Falciano[75a], L.F. Falda Ulhoa Coelho[36], P.J. Falke[24], S. Falke[36], J. Faltova[133], C. Fan[162], Y. Fan[14a], Y. Fang[14a,14e], M. Fanti[71a,71b], M. Faraj[69a,69b], Z. Farazpay[97], A. Farbin[8], A. Farilla[77a], T. Farooque[107], S.M. Farrington[52], F. Fassi[35e], D. Fassouliotis[9], M. Faucci Giannelli[76a,76b], W.J. Fawcett[32], L. Fayard[66], P. Federic[133], P. Federicova[131], O.L. Fedin[37,a], G. Fedotov[37], M. Feickert[170], L. Feligioni[102], A. Fell[139], D.E. Fellers[123], C. Feng[62b], M. Feng[14b], Z. Feng[114], M.J. Fenton[160], A.B. Fenyuk[37], L. Ferencz[48], R.A.M. Ferguson[91], S.I. Fernandez Luengo[137f], M.J.V. Fernoux[102], J. Ferrando[48], A. Ferrari[161], P. Ferrari[114,113], R. Ferrari[73a], D. Ferrere[56], C. Ferretti[106], F. Fiedler[100], A. Filipčič[93], E.K. Filmer[1], F. Filthaut[113], M.C.N. Fiolhais[130a,130c,c], L. Fiorini[163], W.C. Fisher[107], T. Fitschen[101], I. Fleck[141], P. Fleischmann[106], T. Flick[171], L. Flores[128], M. Flores[33d,af], L.R. Flores Castillo[64a], F.M. Follega[78a,78b], N. Fomin[16], J.H. Foo[155], B.C. Forland[68], A. Formica[135], A.C. Forti[101], E. Fortin[36], A.W. Fortman[61], M.G. Foti[17a], L. Fountas[9,k], D. Fournier[66], H. Fox[91], P. Francavilla[74a,74b], S. Francescato[61], S. Franchellucci[56], M. Franchini[23b,23a], S. Franchino[63a], D. Francis[36], L. Franco[113], L. Franconi[48], M. Franklin[61], G. Frattari[26], A.C. Freegard[94], W.S. Freund[82b], Y.Y. Frid[151], N. Fritzsche[50], A. Froch[54], D. Froidevaux[36], J.A. Frost[126], Y. Fu[62a], M. Fujimoto[118], E. Fullana Torregrosa[163,*], E. Furtado De Simas Filho[82b], J. Fuster[163], A. Gabrielli[23b,23a], A. Gabrielli[155], P. Gadow[48], G. Gagliardi[57b,57a], L.G. Gagnon[17a], E.J. Gallas[126], B.J. Gallop[134], K.K. Gan[119], S. Ganguly[153], J. Gao[62a], Y. Gao[52], F.M. Garay Walls[137a,137b], B. Garcia[29,ak], C. García[163], A. Garcia Alonso[114], J.E. García Navarro[163], M. Garcia-Sciveres[17a], R.W. Gardner[39], D. Garg[80], R.B. Garg[143,q], C.A. Garner[155], S.J. Gasiorowski[138], P. Gaspar[82b], G. Gaudio[73a], V. Gautam[13], P. Gauzzi[75a,75b], I.L. Gavrilenko[37], A. Gavrilyuk[37], C. Gay[164], G. Gaycken[48], E.N. Gazis[10], A.A. Geanta[27b,27e], C.M. Gee[136], C. Gemme[57b], M.H. Genest[60], S. Gentile[75a,75b], S. George[95], W.F. George[20], T. Geralis[46], L.O. Gerlach[55], P. Gessinger-Befurt[36], M.E. Geyik[171], M. Ghneimat[141], K. Ghorbanian[94], A. Ghosal[141], A. Ghosh[160], A. Ghosh[7], B. Giacobbe[23b], S. Giagu[75a,75b], P. Giannetti[74a], A. Giannini[62a], S.M. Gibson[95], M. Gignac[136], D.T. Gil[85b], A.K. Gilbert[85a], B.J. Gilbert[41], D. Gillberg[34], G. Gilles[114], N.E.K. Gillwald[48], L. Ginabat[127], D.M. Gingrich[2,ai], M.P. Giordani[69a,69c], P.F. Giraud[135], G. Giugliarelli[69a,69c], D. Giugni[71a], F. Giuli[36], I. Gkialas[9,k], L.K. Gladilin[37],

C. Glasman[99], G.R. Gledhill[123], M. Glisic[123], I. Gnesi[43b,g], Y. Go[29,ak], M. Goblirsch-Kolb[36],
B. Gocke[49], D. Godin[108], B. Gokturk[21a], S. Goldfarb[105], T. Golling[56], M.G.D. Gololo[33g],
D. Golubkov[37], J.P. Gombas[107], A. Gomes[130a,130b], G. Gomes Da Silva[141],
A.J. Gomez Delegido[163], R. Gonçalo[130a,130c], G. Gonella[123], L. Gonella[20], A. Gongadze[38],
F. Gonnella[20], J.L. Gonski[41], R.Y. González Andana[52], S. González de la Hoz[163],
S. Gonzalez Fernandez[13], R. Gonzalez Lopez[92], C. Gonzalez Renteria[17a], R. Gonzalez Suarez[161],
S. Gonzalez-Sevilla[56], G.R. Gonzalvo Rodriguez[163], L. Goossens[36], P.A. Gorbounov[37],
B. Gorini[36], E. Gorini[70a,70b], A. Gorišek[93], T.C. Gosart[128], A.T. Goshaw[51], M.I. Gostkin[38],
S. Goswami[121], C.A. Gottardo[36], M. Gouighri[35b], V. Goumarre[48], A.G. Goussiou[138],
N. Govender[33c], I. Grabowska-Bold[85a], K. Graham[34], E. Gramstad[125], S. Grancagnolo[70a,70b],
M. Grandi[146], V. Gratchev[37,*], P.M. Gravila[27f], F.G. Gravili[70a,70b], H.M. Gray[17a],
M. Greco[70a,70b], C. Grefe[24], I.M. Gregor[48], P. Grenier[143], C. Grieco[13], A.A. Grillo[136],
K. Grimm[31,n], S. Grinstein[13,v], J.-F. Grivaz[66], E. Gross[169], J. Grosse-Knetter[55], C. Grud[106],
J.C. Grundy[126], L. Guan[106], W. Guan[29], C. Gubbels[164], J.G.R. Guerrero Rojas[163],
G. Guerrieri[69a,69b], F. Guescini[110], R. Gugel[100], J.A.M. Guhit[106], A. Guida[48], T. Guillemin[4],
E. Guilloton[167,134], S. Guindon[36], F. Guo[14a,14e], J. Guo[62c], L. Guo[66], Y. Guo[106],
R. Gupta[48], S. Gurbuz[24], S.S. Gurdasani[54], G. Gustavino[36], M. Guth[56], P. Gutierrez[120],
L.F. Gutierrez Zagazeta[128], C. Gutschow[96], C. Gwenlan[126], C.B. Gwilliam[92], E.S. Haaland[125],
A. Haas[117], M. Habedank[48], C. Haber[17a], H.K. Hadavand[8], A. Hadef[100], S. Hadzic[110],
E.H. Haines[96], M. Haleem[166], J. Haley[121], J.J. Hall[139], G.D. Hallewell[102], L. Halser[19],
K. Hamano[165], H. Hamdaoui[35e], M. Hamer[24], G.N. Hamity[52], E.J. Hampshire[95], J. Han[62b],
K. Han[62a], L. Han[14c], L. Han[62a], S. Han[17a], Y.F. Han[155], K. Hanagaki[83], M. Hance[136],
D.A. Hangal[41,ae], H. Hanif[142], M.D. Hank[128], R. Hankache[101], J.B. Hansen[42],
J.D. Hansen[42], P.H. Hansen[42], K. Hara[157], D. Harada[56], T. Harenberg[171], S. Harkusha[37],
Y.T. Harris[126], N.M. Harrison[119], P.F. Harrison[167], N.M. Hartman[143], N.M. Hartmann[109],
Y. Hasegawa[140], A. Hasib[52], S. Haug[19], R. Hauser[107], M. Havranek[132], C.M. Hawkes[20],
R.J. Hawkings[36], S. Hayashida[111], D. Hayden[107], C. Hayes[106], R.L. Hayes[114], C.P. Hays[126],
J.M. Hays[94], H.S. Hayward[92], F. He[62a], Y. He[154], Y. He[127], N.B. Heatley[94],
V. Hedberg[98], A.L. Heggelund[125], N.D. Hehir[94], C. Heidegger[54], K.K. Heidegger[54],
W.D. Heidorn[81], J. Heilman[34], S. Heim[48], T. Heim[17a], J.G. Heinlein[128], J.J. Heinrich[123],
L. Heinrich[110,ag], J. Hejbal[131], L. Helary[48], A. Held[170], S. Hellesund[16], C.M. Helling[164],
S. Hellman[47a,47b], C. Helsens[36], R.C.W. Henderson[91], L. Henkelmann[32],
A.M. Henriques Correia[36], H. Herde[98], Y. Hernández Jiménez[145], L.M. Herrmann[24],
T. Herrmann[50], G. Herten[54], R. Hertenberger[109], L. Hervas[36], N.P. Hessey[156a], H. Hibi[84],
S.J. Hillier[20], F. Hinterkeuser[24], M. Hirose[124], S. Hirose[157], D. Hirschbuehl[171],
T.G. Hitchings[101], B. Hiti[93], J. Hobbs[145], R. Hobincu[27e], N. Hod[169], M.C. Hodgkinson[139],
B.H. Hodkinson[32], A. Hoecker[36], J. Hofer[48], T. Holm[24], M. Holzbock[110],
L.B.A.H. Hommels[32], B.P. Honan[101], J. Hong[62c], T.M. Hong[129], J.C. Honig[54],
B.H. Hooberman[162], W.H. Hopkins[6], Y. Horii[111], S. Hou[148], A.S. Howard[93], J. Howarth[59],
J. Hoya[6], M. Hrabovsky[122], A. Hrynevich[48], T. Hryn'ova[4], P.J. Hsu[65], S.-C. Hsu[138],
Q. Hu[41], Y.F. Hu[14a,14e], D.P. Huang[96], S. Huang[64b], X. Huang[14c], Y. Huang[62a],
Y. Huang[14a], Z. Huang[101], Z. Hubacek[132], M. Huebner[24], F. Huegging[24], T.B. Huffman[126],

M. Huhtinen[36], S.K. Huiberts[16], R. Hulsken[104], N. Huseynov[12,a], J. Huston[107], J. Huth[61], R. Hyneman[143], G. Iacobucci[56], G. Iakovidis[29], I. Ibragimov[141], L. Iconomidou-Fayard[66], P. Iengo[72a,72b], R. Iguchi[153], T. Iizawa[56], Y. Ikegami[83], A. Ilg[19], N. Ilic[155], H. Imam[35a], T. Ingebretsen Carlson[47a,47b], G. Introzzi[73a,73b], M. Iodice[77a], V. Ippolito[75a,75b], M. Ishino[153], W. Islam[170], C. Issever[18,48], S. Istin[21a,am], H. Ito[168], J.M. Iturbe Ponce[64a], R. Iuppa[78a,78b], A. Ivina[169], J.M. Izen[45], V. Izzo[72a], P. Jacka[131,132], P. Jackson[1], R.M. Jacobs[48], B.P. Jaeger[142], C.S. Jagfeld[109], P. Jain[54], G. Jäkel[171], K. Jakobs[54], T. Jakoubek[169], J. Jamieson[59], K.W. Janas[85a], A.E. Jaspan[92], M. Javurkova[103], F. Jeanneau[135], L. Jeanty[123], J. Jejelava[149a,ac], P. Jenni[54,h], C.E. Jessiman[34], S. Jézéquel[4], C. Jia[62b], J. Jia[145], X. Jia[61], X. Jia[14a,14e], Z. Jia[14c], Y. Jiang[62a], S. Jiggins[48], J. Jimenez Pena[110], S. Jin[14c], A. Jinaru[27b], O. Jinnouchi[154], P. Johansson[139], K.A. Johns[7], J.W. Johnson[136], D.M. Jones[32], E. Jones[48], P. Jones[32], R.W.L. Jones[91], T.J. Jones[92], R. Joshi[119], J. Jovicevic[15], X. Ju[17a], J.J. Junggeburth[36], T. Junkermann[63a], A. Juste Rozas[13,v], S. Kabana[137e], A. Kaczmarska[86], M. Kado[110], H. Kagan[119], M. Kagan[143], A. Kahn[41], A. Kahn[128], C. Kahra[100], T. Kaji[168], E. Kajomovitz[150], N. Kakati[169], C.W. Kalderon[29], A. Kamenshchikov[155], S. Kanayama[154], N.J. Kang[136], D. Kar[33g], K. Karava[126], M.J. Kareem[156b], E. Karentzos[54], I. Karkanias[152,f], S.N. Karpov[38], Z.M. Karpova[38], V. Kartvelishvili[91], A.N. Karyukhin[37], E. Kasimi[152,f], J. Katzy[48], S. Kaur[34], K. Kawade[140], T. Kawamoto[135], G. Kawamura[55], E.F. Kay[165], F.I. Kaya[158], S. Kazakos[13], V.F. Kazanin[37], Y. Ke[145], J.M. Keaveney[33a], R. Keeler[165], G.V. Kehris[61], J.S. Keller[34], A.S. Kelly[96], D. Kelsey[146], J.J. Kempster[146], K.E. Kennedy[41], P.D. Kennedy[100], O. Kepka[131], B.P. Kerridge[167], S. Kersten[171], B.P. Kerševan[93], S. Keshri[66], L. Keszeghova[28a], S. Ketabchi Haghighat[155], M. Khandoga[127], A. Khanov[121], A.G. Kharlamov[37], T. Kharlamova[37], E.E. Khoda[138], T.J. Khoo[18], G. Khoriauli[166], J. Khubua[149b], Y.A.R. Khwaira[66], M. Kiehn[36], A. Kilgallon[123], D.W. Kim[47a,47b], Y.K. Kim[39], N. Kimura[96], A. Kirchhoff[55], C. Kirfel[24], J. Kirk[134], A.E. Kiryunin[110], T. Kishimoto[153], D.P. Kisliuk[155], C. Kitsaki[10], O. Kivernyk[24], M. Klassen[63a], C. Klein[34], L. Klein[166], M.H. Klein[106], M. Klein[92], S.B. Klein[56], U. Klein[92], P. Klimek[36], A. Klimentov[29], T. Klioutchnikova[36], P. Kluit[114], S. Kluth[110], E. Kneringer[79], T.M. Knight[155], A. Knue[54], R. Kobayashi[87], M. Kocian[143], P. Kodyš[133], D.M. Koeck[123], P.T. Koenig[24], T. Koffas[34], M. Kolb[135], I. Koletsou[4], T. Komarek[122], K. Köneke[54], A.X.Y. Kong[1], T. Kono[118], N. Konstantinidis[96], B. Konya[98], R. Kopeliansky[68], S. Koperny[85a], K. Korcyl[86], K. Kordas[152,f], G. Koren[151], A. Korn[96], S. Korn[55], I. Korolkov[13], N. Korotkova[37], B. Kortman[114], O. Kortner[110], S. Kortner[110], W.H. Kostecka[115], V.V. Kostyukhin[141], A. Kotsokechagia[135], A. Kotwal[51], A. Koulouris[36], A. Kourkoumeli-Charalampidi[73a,73b], C. Kourkoumelis[9], E. Kourlitis[6], O. Kovanda[146], R. Kowalewski[165], W. Kozanecki[135], A.S. Kozhin[37], V.A. Kramarenko[37], G. Kramberger[93], P. Kramer[100], M.W. Krasny[127], A. Krasznahorkay[36], J.A. Kremer[100], T. Kresse[50], J. Kretzschmar[92], K. Kreul[18], P. Krieger[155], S. Krishnamurthy[103], M. Krivos[133], K. Krizka[20], K. Kroeninger[49], H. Kroha[110], J. Kroll[131], J. Kroll[128], K.S. Krowpman[107], U. Kruchonak[38], H. Krüger[24], N. Krumnack[81], M.C. Kruse[51], J.A. Krzysiak[86], O. Kuchinskaia[37], S. Kuday[3a], S. Kuehn[36], R. Kuesters[54], T. Kuhl[48], V. Kukhtin[38], Y. Kulchitsky[37,a], S. Kuleshov[137d,137b], M. Kumar[33g], N. Kumari[102], A. Kupco[131], T. Kupfer[49], A. Kupich[37], O. Kuprash[54],

H. Kurashige[84], L.L. Kurchaninov[156a], O. Kurdysh[66], Y.A. Kurochkin[37], A. Kurova[37], M. Kuze[154], A.K. Kvam[103], J. Kvita[122], T. Kwan[104], N.G. Kyriacou[106], L.A.O. Laatu[102], C. Lacasta[163], F. Lacava[75a,75b], H. Lacker[18], D. Lacour[127], N.N. Lad[96], E. Ladygin[38], B. Laforge[127], T. Lagouri[137e], S. Lai[55], I.K. Lakomiec[85a], N. Lalloue[60], J.E. Lambert[120], S. Lammers[68], W. Lampl[7], C. Lampoudis[152,f], A.N. Lancaster[115], E. Lançon[29], U. Landgraf[54], M.P.J. Landon[94], V.S. Lang[54], R.J. Langenberg[103], A.J. Lankford[160], F. Lanni[36], K. Lantzsch[24], A. Lanza[73a], A. Lapertosa[57b,57a], J.F. Laporte[135], T. Lari[71a], F. Lasagni Manghi[23b], M. Lassnig[36], V. Latonova[131], A. Laudrain[100], A. Laurier[150], S.D. Lawlor[95], Z. Lawrence[101], M. Lazzaroni[71a,71b], B. Le[101], E.M. Le Boulicaut[51], B. Leban[93], A. Lebedev[81], M. LeBlanc[36], F. Ledroit-Guillon[60], A.C.A. Lee[96], G.R. Lee[16], S.C. Lee[148], S. Lee[47a,47b], T.F. Lee[92], L.L. Leeuw[33c], H.P. Lefebvre[95], M. Lefebvre[165], C. Leggett[17a], K. Lehmann[142], G. Lehmann Miotto[36], M. Leigh[56], W.A. Leight[103], A. Leisos[152,u], M.A.L. Leite[82c], C.E. Leitgeb[48], R. Leitner[133], K.J.C. Leney[44], T. Lenz[24], S. Leone[74a], C. Leonidopoulos[52], A. Leopold[144], C. Leroy[108], R. Les[107], C.G. Lester[32], M. Levchenko[37], J. Levêque[4], D. Levin[106], L.J. Levinson[169], M.P. Lewicki[86], D.J. Lewis[4], A. Li[5], B. Li[62b], C. Li[62a], C-Q. Li[62c], H. Li[62a], H. Li[62b], H. Li[14c], H. Li[62b], J. Li[62c], K. Li[138], L. Li[62c], M. Li[14a,14e], Q.Y. Li[62a], S. Li[14a,14e], S. Li[62d,62c,e], T. Li[62b], X. Li[104], Z. Li[62b], Z. Li[126], Z. Li[104], Z. Li[92], Z. Li[14a,14e], Z. Liang[14a], M. Liberatore[48], B. Liberti[76a], K. Lie[64c], J. Lieber Marin[82b], H. Lien[68], K. Lin[107], R.A. Linck[68], R.E. Lindley[7], J.H. Lindon[2], A. Linss[48], E. Lipeles[128], A. Lipniacka[16], A. Lister[164], J.D. Little[4], B. Liu[14a], B.X. Liu[142], D. Liu[62d,62c], J.B. Liu[62a], J.K.K. Liu[32], K. Liu[62d,62c], M. Liu[62a], M.Y. Liu[62a], P. Liu[14a], Q. Liu[62d,138,62c], X. Liu[62a], Y. Liu[14d,14e], Y.L. Liu[106], Y.W. Liu[62a], J. Llorente Merino[142], S.L. Lloyd[94], E.M. Lobodzinska[48], P. Loch[7], S. Loffredo[76a,76b], T. Lohse[18], K. Lohwasser[139], E. Loiacono[48], M. Lokajicek[131,*], J.D. Lomas[20], J.D. Long[162], I. Longarini[160], L. Longo[70a,70b], R. Longo[162], I. Lopez Paz[67], A. Lopez Solis[48], J. Lorenz[109], N. Lorenzo Martinez[4], A.M. Lory[109], X. Lou[47a,47b], X. Lou[14a,14e], A. Lounis[66], J. Love[6], P.A. Love[91], G. Lu[14a,14e], M. Lu[80], S. Lu[128], Y.J. Lu[65], H.J. Lubatti[138], C. Luci[75a,75b], F.L. Lucio Alves[14c], A. Lucotte[60], F. Luehring[68], I. Luise[145], O. Lukianchuk[66], O. Lundberg[144], B. Lund-Jensen[144], N.A. Luongo[123], M.S. Lutz[151], D. Lynn[29], H. Lyons[92], R. Lysak[131], E. Lytken[98], V. Lyubushkin[38], T. Lyubushkina[38], M.M. Lyukova[145], H. Ma[29], L.L. Ma[62b], Y. Ma[96], D.M. Mac Donell[165], G. Maccarrone[53], J.C. MacDonald[139], R. Madar[40], W.F. Mader[50], J. Maeda[84], T. Maeno[29], M. Maerker[50], H. Maguire[139], A. Maio[130a,130b,130d], K. Maj[85a], O. Majersky[48], S. Majewski[123], N. Makovec[66], V. Maksimovic[15], B. Malaescu[127], Pa. Malecki[86], V.P. Maleev[37], F. Malek[60], D. Malito[43b,43a], U. Mallik[80], C. Malone[32], S. Maltezos[10], S. Malyukov[38], J. Mamuzic[13], G. Mancini[53], G. Manco[73a,73b], J.P. Mandalia[94], I. Mandić[93], L. Manhaes de Andrade Filho[82a], I.M. Maniatis[169], J. Manjarres Ramos[102,ad], D.C. Mankad[169], A. Mann[109], B. Mansoulie[135], S. Manzoni[36], A. Marantis[152,u], G. Marchiori[5], M. Marcisovsky[131], C. Marcon[71a,71b], M. Marinescu[20], M. Marjanovic[120], E.J. Marshall[91], Z. Marshall[17a], S. Marti-Garcia[163], T.A. Martin[167], V.J. Martin[52], B. Martin dit Latour[16], L. Martinelli[75a,75b], M. Martinez[13,v], P. Martinez Agullo[163], V.I. Martinez Outschoorn[103], P. Martinez Suarez[13], S. Martin-Haugh[134], V.S. Martoiu[27b], A.C. Martyniuk[96], A. Marzin[36], S.R. Maschek[110], D. Mascione[78a,78b], L. Masetti[100], T. Mashimo[153], J. Masik[101], A.L. Maslennikov[37], L. Massa[23b], P. Massarotti[72a,72b], P. Mastrandrea[74a,74b], A. Mastroberardino[43b,43a], T. Masubuchi[153], T. Mathisen[161], N. Matsuzawa[153], J. Maurer[27b], B. Maček[93], D.A. Maximov[37], R. Mazini[148], I. Maznas[152,f], M. Mazza[107], S.M. Mazza[136], C. Mc Ginn[29], J.P. Mc Gowan[104], S.P. Mc Kee[106], E.F. McDonald[105], A.E. McDougall[114], J.A. Mcfayden[146], R.P. McGovern[128], G. Mchedlidze[149b], R.P. Mckenzie[33g], T.C. Mclachlan[48], D.J. Mclaughlin[96], K.D. McLean[165], S.J. McMahon[134], P.C. McNamara[105], C.M. Mcpartland[92], R.A. McPherson[165,z], T. Megy[40], S. Mehlhase[109], A. Mehta[92], D. Melini[150], B.R. Mellado Garcia[33g], A.H. Melo[55], F. Meloni[48], A.M. Mendes Jacques Da Costa[101], H.Y. Meng[155], L. Meng[91], S. Menke[110], M. Mentink[36], E. Meoni[43b,43a], C. Merlassino[126], L. Merola[72a,72b], C. Meroni[71a,71b], G. Merz[106], O. Meshkov[37], J. Metcalfe[6], A.S. Mete[6], C. Meyer[68], J-P. Meyer[135], R.P. Middleton[134], L. Mijović[52], G. Mikenberg[169], M. Mikestikova[131], M. Mikuž[93], H. Mildner[139], A. Milic[36], C.D. Milke[44], D.W. Miller[39], L.S. Miller[34], A. Milov[169], D.A. Milstead[47a,47b], T. Min[14c], A.A. Minaenko[37], I.A. Minashvili[149b], L. Mince[59], A.I. Mincer[117], B. Mindur[85a], M. Mineev[38], Y. Mino[87], L.M. Mir[13], M. Miralles Lopez[163], M. Mironova[17a], M.C. Missio[113], T. Mitani[168], A. Mitra[167], V.A. Mitsou[163], O. Miu[155], P.S. Miyagawa[94], Y. Miyazaki[89], A. Mizukami[83], T. Mkrtchyan[63a], M. Mlinarevic[96], T. Mlinarevic[96], M. Mlynarikova[36], S. Mobius[55], K. Mochizuki[108], P. Moder[48], P. Mogg[109], A.F. Mohammed[14a,14e], S. Mohapatra[41], G. Mokgatitswane[33g], B. Mondal[141], S. Mondal[132], G. Monig[146], K. Mönig[48], E. Monnier[102], L. Monsonis Romero[163], J. Montejo Berlingen[83], M. Montella[119], F. Monticelli[90], N. Morange[66], A.L. Moreira De Carvalho[130a], M. Moreno Llácer[163], C. Moreno Martinez[56], P. Morettini[57b], S. Morgenstern[36], M. Morii[61], M. Morinaga[153], A.K. Morley[36], F. Morodei[75a,75b], L. Morvaj[36], P. Moschovakos[36], B. Moser[36], M. Mosidze[149b], T. Moskalets[54], P. Moskvitina[113], J. Moss[31,o], E.J.W. Moyse[103], O. Mtintsilana[33g], S. Muanza[102], J. Mueller[129], D. Muenstermann[91], R. Müller[19], G.A. Mullier[161], J.J. Mullin[128], D.P. Mungo[155], J.L. Munoz Martinez[13], D. Munoz Perez[163], F.J. Munoz Sanchez[101], M. Murin[101], W.J. Murray[167,134], A. Murrone[71a,71b], J.M. Muse[120], M. Muškinja[17a], C. Mwewa[29], A.G. Myagkov[37,a], A.J. Myers[8], A.A. Myers[129], G. Myers[68], M. Myska[132], B.P. Nachman[17a], O. Nackenhorst[49], A. Nag[50], K. Nagai[126], K. Nagano[83], J.L. Nagle[29,ak], E. Nagy[102], A.M. Nairz[36], Y. Nakahama[83], K. Nakamura[83], H. Nanjo[124], R. Narayan[44], E.A. Narayanan[112], I. Naryshkin[37], M. Naseri[34], C. Nass[24], G. Navarro[22a], J. Navarro-Gonzalez[163], R. Nayak[151], A. Nayaz[18], P.Y. Nechaeva[37], F. Nechansky[48], L. Nedic[126], T.J. Neep[20], A. Negri[73a,73b], M. Negrini[23b], C. Nellist[114], C. Nelson[104], K. Nelson[106], S. Nemecek[131], M. Nessi[36,i], M.S. Neubauer[162], F. Neuhaus[100], J. Neundorf[48], R. Newhouse[164], P.R. Newman[20], C.W. Ng[129], Y.W.Y. Ng[48], B. Ngair[35e], H.D.N. Nguyen[108], R.B. Nickerson[126], R. Nicolaidou[135], J. Nielsen[136], M. Niemeyer[55], N. Nikiforou[36], V. Nikolaenko[37,a], I. Nikolic-Audit[127], K. Nikolopoulos[20], P. Nilsson[29], I. Ninca[48], H.R. Nindhito[56], G. Ninio[151], A. Nisati[75a], N. Nishu[2], R. Nisius[110], J-E. Nitschke[50], E.K. Nkadimeng[33g], S.J. Noacco Rosende[90], T. Nobe[153], D.L. Noel[32], T. Nommensen[147], M.A. Nomura[29], M.B. Norfolk[139], R.R.B. Norisam[96], B.J. Norman[34], J. Novak[93], T. Novak[48], L. Novotny[132], R. Novotny[112], L. Nozka[122], K. Ntekas[160], N.M.J. Nunes De Moura Junior[82b], E. Nurse[96], J. Ocariz[127], A. Ochi[84], I. Ochoa[130a], S. Oerdek[161], J.T. Offermann[39], A. Ogrodnik[85a], A. Oh[101], C.C. Ohm[144], H. Oide[83], R. Oishi[153], M.L. Ojeda[48], Y. Okazaki[87], M.W. O'Keefe[92], Y. Okumura[153], L.F. Oleiro Seabra[130a], S.A. Olivares Pino[137d], D. Oliveira Damazio[29], D. Oliveira Goncalves[82a], J.L. Oliver[160], M.J.R. Olsson[160], A. Olszewski[86], Ö.O. Öncel[54], D.C. O'Neil[142], A.P. O'Neill[19], A. Onofre[130a,130e], P.U.E. Onyisi[11], M.J. Oreglia[39], G.E. Orellana[90], D. Orestano[77a,77b], N. Orlando[13], R.S. Orr[155], V. O'Shea[59], R. Ospanov[62a], G. Otero y Garzon[30], H. Otono[89], P.S. Ott[63a], G.J. Ottino[17a], M. Ouchrif[35d], J. Ouellette[29], F. Ould-Saada[125], M. Owen[59], R.E. Owen[134], K.Y. Oyulmaz[21a], V.E. Ozcan[21a], N. Ozturk[8], S. Ozturk[21d], H.A. Pacey[32], A. Pacheco Pages[13], C. Padilla Aranda[13], G. Padovano[75a,75b], S. Pagan Griso[17a], G. Palacino[68], A. Palazzo[70a,70b], S. Palestini[36], J. Pan[172], T. Pan[64a], D.K. Panchal[11], C.E. Pandini[114], J.G. Panduro Vazquez[95], H. Pang[14b], P. Pani[48], G. Panizzo[69a,69c], L. Paolozzi[56], C. Papadatos[108], S. Parajuli[44], A. Paramonov[6], C. Paraskevopoulos[10], D. Paredes Hernandez[64b], T.H. Park[155], M.A. Parker[32], F. Parodi[57b,57a], E.W. Parrish[115], V.A. Parrish[52], J.A. Parsons[41], U. Parzefall[54], B. Pascual Dias[108], L. Pascual Dominguez[151], F. Pasquali[114], E. Pasqualucci[75a], S. Passaggio[57b], F. Pastore[95], P. Pasuwan[47a,47b], P. Patel[86], U.M. Patel[51], J.R. Pater[101], T. Pauly[36], J. Pearkes[143], M. Pedersen[125], R. Pedro[130a], S.V. Peleganchuk[37], O. Penc[36], E.A. Pender[52], H. Peng[62a], K.E. Penski[109], M. Penzin[37], B.S. Peralva[82d], A.P. Pereira Peixoto[60], L. Pereira Sanchez[47a,47b], D.V. Perepelitsa[29,ak], E. Perez Codina[156a], M. Perganti[10], L. Perini[71a,71b,*], H. Pernegger[36], A. Perrevoort[113], O. Perrin[40], K. Peters[48], R.F.Y. Peters[101], B.A. Petersen[36], T.C. Petersen[42], E. Petit[102], V. Petousis[132], C. Petridou[152,f], A. Petrukhin[141], M. Pettee[17a], N.E. Pettersson[36], A. Petukhov[37], K. Petukhova[133], A. Peyaud[135], R. Pezoa[137f], L. Pezzotti[36], G. Pezzullo[172], T.M. Pham[170], T. Pham[105], P.W. Phillips[134], M.W. Phipps[162], G. Piacquadio[145], E. Pianori[17a], F. Piazza[71a,71b], R. Piegaia[30], D. Pietreanu[27b], A.D. Pilkington[101], M. Pinamonti[69a,69c], J.L. Pinfold[2], B.C. Pinheiro Pereira[130a], C. Pitman Donaldson[96], D.A. Pizzi[34], L. Pizzimento[76a,76b], A. Pizzini[114], M.-A. Pleier[29], V. Plesanovs[54], V. Pleskot[133], E. Plotnikova[38], G. Poddar[4], R. Poettgen[98], L. Poggioli[127], D. Pohl[24], I. Pokharel[55], S. Polacek[133], G. Polesello[73a], A. Poley[142,156a], R. Polifka[132], A. Polini[23b], C.S. Pollard[167], Z.B. Pollock[119], V. Polychronakos[29], E. Pompa Pacchi[75a,75b], D. Ponomarenko[113], L. Pontecorvo[36], S. Popa[27a], G.A. Popeneciu[27d], D.M. Portillo Quintero[156a], S. Pospisil[132], P. Postolache[27c], K. Potamianos[126], P.A. Potepa[85a], I.N. Potrap[38], C.J. Potter[32], H. Potti[1], T. Poulsen[48], J. Poveda[163], M.E. Pozo Astigarraga[36], A. Prades Ibanez[163], M.M. Prapa[46], J. Pretel[54], D. Price[101], M. Primavera[70a], M.A. Principe Martin[99], R. Privara[122], M.L. Proffitt[138], N. Proklova[128], K. Prokofiev[64c], G. Proto[76a,76b], S. Protopopescu[29], J. Proudfoot[6], M. Przybycien[85a], W.W. Przygoda[85b], J.E. Puddefoot[139], D. Pudzha[37], D. Pyatiizbyantseva[37], J. Qian[106], D. Qichen[101], Y. Qin[101], T. Qiu[52], A. Quadt[55], M. Queitsch-Maitland[101], G. Quetant[56], G. Rabanal Bolanos[61], D. Rafanoharana[54], F. Ragusa[71a,71b], J.L. Rainbolt[39], J.A. Raine[56], S. Rajagopalan[29], E. Ramakoti[37], K. Ran[48,14e], N.P. Rapheeha[33g], V. Raskina[127], D.F. Rassloff[63a], S. Rave[100], B. Ravina[55], I. Ravinovich[169], M. Raymond[36], A.L. Read[125], N.P. Readioff[139], D.M. Rebuzzi[73a,73b], G. Redlinger[29], K. Reeves[26], J.A. Reidelsturz[171], D. Reikher[151],

A. Rej[141], C. Rembser[36], A. Renardi[48], M. Renda[27b], M.B. Rendel[110], F. Renner[48], A.G. Rennie[59], S. Resconi[71a], M. Ressegotti[57b,57a], E.D. Resseguie[17a], S. Rettie[36], J.G. Reyes Rivera[107], B. Reynolds[119], E. Reynolds[17a], M. Rezaei Estabragh[171], O.L. Rezanova[37], P. Reznicek[133], N. Ribaric[91], E. Ricci[78a,78b], R. Richter[110], S. Richter[47a,47b], E. Richter-Was[85b], M. Ridel[127], S. Ridouani[35d], P. Rieck[117], P. Riedler[36], M. Rijssenbeek[145], A. Rimoldi[73a,73b], M. Rimoldi[48], L. Rinaldi[23b,23a], T.T. Rinn[29], M.P. Rinnagel[109], G. Ripellino[161], I. Riu[13], P. Rivadeneira[48], J.C. Rivera Vergara[165], F. Rizatdinova[121], E. Rizvi[94], C. Rizzi[56], B.A. Roberts[167], B.R. Roberts[17a], S.H. Robertson[104,z], M. Robin[48], D. Robinson[32], C.M. Robles Gajardo[137f], M. Robles Manzano[100], A. Robson[59], A. Rocchi[76a,76b], C. Roda[74a,74b], S. Rodriguez Bosca[63a], Y. Rodriguez Garcia[22a], A. Rodriguez Rodriguez[54], A.M. Rodríguez Vera[156b], S. Roe[36], J.T. Roemer[160], A.R. Roepe-Gier[136], J. Roggel[171], O. Røhne[125], R.A. Rojas[103], C.P.A. Roland[68], J. Roloff[29], A. Romaniouk[37], E. Romano[73a,73b], M. Romano[23b], A.C. Romero Hernandez[162], N. Rompotis[92], L. Roos[127], S. Rosati[75a], B.J. Rosser[39], E. Rossi[4], E. Rossi[72a,72b], L.P. Rossi[57b], L. Rossini[48], R. Rosten[119], M. Rotaru[27b], B. Rottler[54], C. Rougier[102,ad], D. Rousseau[66], D. Rousso[32], A. Roy[162], S. Roy-Garand[155], A. Rozanov[102], Y. Rozen[150], X. Ruan[33g], A. Rubio Jimenez[163], A.J. Ruby[92], V.H. Ruelas Rivera[18], T.A. Ruggeri[1], A. Ruggiero[126], A. Ruiz-Martinez[163], A. Rummler[36], Z. Rurikova[54], N.A. Rusakovich[38], H.L. Russell[165], J.P. Rutherfoord[7], K. Rybacki[91], M. Rybar[133], E.B. Rye[125], A. Ryzhov[37], J.A. Sabater Iglesias[56], P. Sabatini[163], L. Sabetta[75a,75b], H.F-W. Sadrozinski[136], F. Safai Tehrani[75a], B. Safarzadeh Samani[146], M. Safdari[143], S. Saha[104], M. Sahinsoy[110], M. Saimpert[135], M. Saito[153], T. Saito[153], D. Salamani[36], A. Salnikov[143], J. Salt[163], A. Salvador Salas[13], D. Salvatore[43b,43a], F. Salvatore[146], A. Salzburger[36], D. Sammel[54], D. Sampsonidis[152,f], D. Sampsonidou[123,62c], J. Sánchez[163], A. Sanchez Pineda[4], V. Sanchez Sebastian[163], H. Sandaker[125], C.O. Sander[48], J.A. Sandesara[103], M. Sandhoff[171], C. Sandoval[22b], D.P.C. Sankey[134], T. Sano[87], A. Sansoni[53], L. Santi[75a,75b], C. Santoni[40], H. Santos[130a,130b], S.N. Santpur[17a], A. Santra[169], K.A. Saoucha[139], J.G. Saraiva[130a,130d], J. Sardain[7], O. Sasaki[83], K. Sato[157], C. Sauer[63b], F. Sauerburger[54], E. Sauvan[4], P. Savard[155,ai], R. Sawada[153], C. Sawyer[134], L. Sawyer[97], I. Sayago Galvan[163], C. Sbarra[23b], A. Sbrizzi[23b,23a], T. Scanlon[96], J. Schaarschmidt[138], P. Schacht[110], D. Schaefer[39], U. Schäfer[100], A.C. Schaffer[66,44], D. Schaile[109], R.D. Schamberger[145], E. Schanet[109], C. Scharf[18], M.M. Schefer[19], V.A. Schegelsky[37], D. Scheirich[133], F. Schenck[18], M. Schernau[160], C. Scheulen[55], C. Schiavi[57b,57a], E.J. Schioppa[70a,70b], M. Schioppa[43b,43a], B. Schlag[143,q], K.E. Schleicher[54], S. Schlenker[36], J. Schmeing[171], M.A. Schmidt[171], K. Schmieden[100], C. Schmitt[100], S. Schmitt[48], L. Schoeffel[135], A. Schoening[63b], P.G. Scholer[54], E. Schopf[126], M. Schott[100], J. Schovancova[36], S. Schramm[56], F. Schroeder[171], H-C. Schultz-Coulon[63a], M. Schumacher[54], B.A. Schumm[136], Ph. Schune[135], H.R. Schwartz[136], A. Schwartzman[143], T.A. Schwarz[106], Ph. Schwemling[135], R. Schwienhorst[107], A. Sciandra[136], G. Sciolla[26], F. Scuri[74a], F. Scutti[105], C.D. Sebastiani[92], K. Sedlaczek[49], P. Seema[18], S.C. Seidel[112], A. Seiden[136], B.D. Seidlitz[41], C. Seitz[48], J.M. Seixas[82b], G. Sekhniaidze[72a], S.J. Sekula[44], L. Selem[4], N. Semprini-Cesari[23b,23a], S. Sen[51], D. Sengupta[56], V. Senthilkumar[163], L. Serin[66],

L. Serkin [69a,69b], M. Sessa [77a,77b], H. Severini [120], F. Sforza [57b,57a], A. Sfyrla [56], E. Shabalina [55], R. Shaheen [144], J.D. Shahinian [128], D. Shaked Renous [169], L.Y. Shan [14a], M. Shapiro [17a], A. Sharma [36], A.S. Sharma [164], P. Sharma [80], S. Sharma [48], P.B. Shatalov [37], K. Shaw [146], S.M. Shaw [101], Q. Shen [62c,5], P. Sherwood [96], L. Shi [96], C.O. Shimmin [172], Y. Shimogama [168], J.D. Shinner [95], I.P.J. Shipsey [126], S. Shirabe [60], M. Shiyakova [38,x], J. Shlomi [169], M.J. Shochet [39], J. Shojaii [105], D.R. Shope [125], S. Shrestha [119,al], E.M. Shrif [33g], M.J. Shroff [165], P. Sicho [131], A.M. Sickles [162], E. Sideras Haddad [33g], A. Sidoti [23b], F. Siegert [50], Dj. Sijacki [15], R. Sikora [85a], F. Sili [90], J.M. Silva [20], M.V. Silva Oliveira [36], S.B. Silverstein [47a], S. Simion [66], R. Simoniello [36], E.L. Simpson [59], H. Simpson [146], L.R. Simpson [106], N.D. Simpson [98], S. Simsek [21d], S. Sindhu [55], P. Sinervo [155], S. Singh [142], S. Singh [155], S. Sinha [48], S. Sinha [33g], M. Sioli [23b,23a], I. Siral [36], S.Yu. Sivoklokov [37,*], J. Sjölin [47a,47b], A. Skaf [55], E. Skorda [98], P. Skubic [120], M. Slawinska [86], V. Smakhtin [169], B.H. Smart [134], J. Smiesko [36], S.Yu. Smirnov [37], Y. Smirnov [37], L.N. Smirnova [37,a], O. Smirnova [98], A.C. Smith [41], E.A. Smith [39], H.A. Smith [126], J.L. Smith [92], R. Smith [143], M. Smizanska [91], K. Smolek [132], A.A. Snesarev [37], H.L. Snoek [114], S. Snyder [29], R. Sobie [165,z], A. Soffer [151], C.A. Solans Sanchez [36], E.Yu. Soldatov [37], U. Soldevila [163], A.A. Solodkov [37], S. Solomon [54], A. Soloshenko [38], K. Solovieva [54], O.V. Solovyanov [40], V. Solovyev [37], P. Sommer [36], A. Sonay [13], W.Y. Song [156b], J.M. Sonneveld [114], A. Sopczak [132], A.L. Sopio [96], F. Sopkova [28b], V. Sothilingam [63a], S. Sottocornola [68], R. Soualah [116b], Z. Soumaimi [35e], D. South [48], S. Spagnolo [70a,70b], M. Spalla [110], D. Sperlich [54], G. Spigo [36], M. Spina [146], S. Spinali [91], D.P. Spiteri [59], M. Spousta [133], E.J. Staats [34], A. Stabile [71a,71b], R. Stamen [63a], M. Stamenkovic [114], A. Stampekis [20], M. Standke [24], E. Stanecka [86], M.V. Stange [50], B. Stanislaus [17a], M.M. Stanitzki [48], M. Stankaityte [126], B. Stapf [48], E.A. Starchenko [37], G.H. Stark [136], J. Stark [102,ad], D.M. Starko [156b], P. Staroba [131], P. Starovoitov [63a], S. Stärz [104], R. Staszewski [86], G. Stavropoulos [46], J. Steentoft [161], P. Steinberg [29], B. Stelzer [142,156a], H.J. Stelzer [129], O. Stelzer-Chilton [156a], H. Stenzel [58], T.J. Stevenson [146], G.A. Stewart [36], J.R. Stewart [121], M.C. Stockton [36], G. Stoicea [27b], M. Stolarski [130a], S. Stonjek [110], A. Straessner [50], J. Strandberg [144], S. Strandberg [47a,47b], M. Strauss [120], T. Strebler [102], P. Strizenec [28b], R. Ströhmer [166], D.M. Strom [123], L.R. Strom [48], R. Stroynowski [44], A. Strubig [47a,47b], S.A. Stucci [29], B. Stugu [16], J. Stupak [120], N.A. Styles [48], D. Su [143], S. Su [62a], W. Su [62d,138,62c], X. Su [62a,66], K. Sugizaki [153], V.V. Sulin [37], M.J. Sullivan [92], D.M.S. Sultan [78a,78b], L. Sultanaliyeva [37], S. Sultansoy [3b], T. Sumida [87], S. Sun [106], S. Sun [170], O. Sunneborn Gudnadottir [161], M.R. Sutton [146], M. Svatos [131], M. Swiatlowski [156a], T. Swirski [166], I. Sykora [28a], M. Sykora [133], T. Sykora [133], D. Ta [100], K. Tackmann [48,w], A. Taffard [160], R. Tafirout [156a], J.S. Tafoya Vargas [66], R.H.M. Taibah [127], R. Takashima [88], E.P. Takeva [52], Y. Takubo [83], M. Talby [102], A.A. Talyshev [37], K.C. Tam [64b], N.M. Tamir [151], A. Tanaka [153], J. Tanaka [153], R. Tanaka [66], M. Tanasini [57b,57a], Z. Tao [164], S. Tapia Araya [137f], S. Tapprogge [100], A. Tarek Abouelfadl Mohamed [107], S. Tarem [150], K. Tariq [62b], G. Tarna [102,27b], G.F. Tartarelli [71a], P. Tas [133], M. Tasevsky [131], E. Tassi [43b,43a], A.C. Tate [162], G. Tateno [153], Y. Tayalati [35e,y], G.N. Taylor [105], W. Taylor [156b], H. Teagle [92], A.S. Tee [170], R. Teixeira De Lima [143], P. Teixeira-Dias [95], J.J. Teoh [155], K. Terashi [153], J. Terron [99], S. Terzo [13], M. Testa [53], R.J. Teuscher [155,z], A. Thaler [79], O. Theiner [56], N. Themistokleous [52],

T. Theveneaux-Pelzer[102], O. Thielmann[171], D.W. Thomas[95], J.P. Thomas[20], E.A. Thompson[17a], P.D. Thompson[20], E. Thomson[128], Y. Tian[55], V. Tikhomirov[37,a], Yu.A. Tikhonov[37], S. Timoshenko[37], E.X.L. Ting[1], P. Tipton[172], S.H. Tlou[33g], A. Tnourji[40], K. Todome[23b,23a], S. Todorova-Nova[133], S. Todt[50], M. Togawa[83], J. Tojo[89], S. Tokár[28a], K. Tokushuku[83], O. Toldaiev[68], R. Tombs[32], M. Tomoto[83,111], L. Tompkins[143,q], K.W. Topolnicki[85b], E. Torrence[123], H. Torres[102,ad], E. Torró Pastor[163], M. Toscani[30], C. Tosciri[39], M. Tost[11], D.R. Tovey[139], A. Traeet[16], I.S. Trandafir[27b], T. Trefzger[166], A. Tricoli[29], I.M. Trigger[156a], S. Trincaz-Duvoid[127], D.A. Trischuk[26], B. Trocmé[60], C. Troncon[71a], L. Truong[33c], M. Trzebinski[86], A. Trzupek[86], F. Tsai[145], M. Tsai[106], A. Tsiamis[152,f], P.V. Tsiareshka[37], S. Tsigaridas[156a], A. Tsirigotis[152,u], V. Tsiskaridze[145], E.G. Tskhadadze[149a], M. Tsopoulou[152,f], Y. Tsujikawa[87], I.I. Tsukerman[37], V. Tsulaia[17a], S. Tsuno[83], O. Tsur[150], D. Tsybychev[145], Y. Tu[64b], A. Tudorache[27b], V. Tudorache[27b], A.N. Tuna[36], S. Turchikhin[38], I. Turk Cakir[3a], R. Turra[71a], T. Turtuvshin[38,aa], P.M. Tuts[41], S. Tzamarias[152,f], P. Tzanis[10], E. Tzovara[100], K. Uchida[153], F. Ukegawa[157], P.A. Ulloa Poblete[137c], E.N. Umaka[29], G. Unal[36], M. Unal[11], A. Undrus[29], G. Unel[160], J. Urban[28b], P. Urquijo[105], G. Usai[8], R. Ushioda[154], M. Usman[108], Z. Uysal[21b], L. Vacavant[102], V. Vacek[132], B. Vachon[104], K.O.H. Vadla[125], T. Vafeiadis[36], A. Vaitkus[96], C. Valderanis[109], E. Valdes Santurio[47a,47b], M. Valente[156a], S. Valentinetti[23b,23a], A. Valero[163], E. Valiente Moreno[163], A. Vallier[102,ad], J.A. Valls Ferrer[163], D.R. Van Arneman[114], T.R. Van Daalen[138], P. Van Gemmeren[6], M. Van Rijnbach[125,36], S. Van Stroud[96], I. Van Vulpen[114], M. Vanadia[76a,76b], W. Vandelli[36], M. Vandenbroucke[135], E.R. Vandewall[121], D. Vannicola[151], L. Vannoli[57b,57a], R. Vari[75a], E.W. Varnes[7], C. Varni[17a], T. Varol[148], D. Varouchas[66], L. Varriale[163], K.E. Varvell[147], M.E. Vasile[27b], L. Vaslin[40], G.A. Vasquez[165], F. Vazeille[40], T. Vazquez Schroeder[36], J. Veatch[31], V. Vecchio[101], M.J. Veen[103], I. Veliscek[126], L.M. Veloce[155], F. Veloso[130a,130c], S. Veneziano[75a], A. Ventura[70a,70b], A. Verbytskyi[110], M. Verducci[74a,74b], C. Vergis[24], M. Verissimo De Araujo[82b], W. Verkerke[114], J.C. Vermeulen[114], C. Vernieri[143], P.J. Verschuuren[95], M. Vessella[103], M.C. Vetterli[142,ai], A. Vgenopoulos[152,f], N. Viaux Maira[137f], T. Vickey[139], O.E. Vickey Boeriu[139], G.H.A. Viehhauser[126], L. Vigani[63b], M. Villa[23b,23a], M. Villaplana Perez[163], E.M. Villhauer[52], E. Vilucchi[53], M.G. Vincter[34], G.S. Virdee[20], A. Vishwakarma[52], C. Vittori[36], I. Vivarelli[146], V. Vladimirov[167], E. Voevodina[110], F. Vogel[109], P. Vokac[132], J. Von Ahnen[48], E. Von Toerne[24], B. Vormwald[36], V. Vorobel[133], K. Vorobev[37], M. Vos[163], K. Voss[141], J.H. Vossebeld[92], M. Vozak[114], L. Vozdecky[94], N. Vranjes[15], M. Vranjes Milosavljevic[15], M. Vreeswijk[114], R. Vuillermet[36], O. Vujinovic[100], I. Vukotic[39], S. Wada[157], C. Wagner[103], J.M. Wagner[17a], W. Wagner[171], S. Wahdan[171], H. Wahlberg[90], R. Wakasa[157], M. Wakida[111], J. Walder[134], R. Walker[109], W. Walkowiak[141], A. Wall[128], A.Z. Wang[170], C. Wang[100], C. Wang[62c], H. Wang[17a], J. Wang[64a], R.-J. Wang[100], R. Wang[61], R. Wang[6], S.M. Wang[148], S. Wang[62b], T. Wang[62a], W.T. Wang[80], X. Wang[14c], X. Wang[162], X. Wang[62c], Y. Wang[62d], Y. Wang[14c], Z. Wang[106], Z. Wang[62d,51,62c], Z. Wang[106], A. Warburton[104], R.J. Ward[20], N. Warrack[59], A.T. Watson[20], H. Watson[59], M.F. Watson[20], G. Watts[138], B.M. Waugh[96], C. Weber[29], H.A. Weber[18], M.S. Weber[19], S.M. Weber[63a], C. Wei[62a],

Y. Wei[126], A.R. Weidberg[126], E.J. Weik[117], J. Weingarten[49], M. Weirich[100], C. Weiser[54], C.J. Wells[48], T. Wenaus[29], B. Wendland[49], T. Wengler[36], N.S. Wenke[110], N. Wermes[24], M. Wessels[63a], K. Whalen[123], A.M. Wharton[91], A.S. White[61], A. White[8], M.J. White[1], D. Whiteson[160], L. Wickremasinghe[124], W. Wiedenmann[170], C. Wiel[50], M. Wielers[134], C. Wiglesworth[42], L.A.M. Wiik-Fuchs[54], D.J. Wilbern[120], H.G. Wilkens[36], D.M. Williams[41], H.H. Williams[128], S. Williams[32], S. Willocq[103], B.J. Wilson[101], P.J. Windischhofer[39], F. Winklmeier[123], B.T. Winter[54], J.K. Winter[101], M. Wittgen[143], M. Wobisch[97], R. Wölker[126], J. Wollrath[160], M.W. Wolter[86], H. Wolters[130a,130c], V.W.S. Wong[164], A.F. Wongel[48], S.D. Worm[48], B.K. Wosiek[86], K.W. Woźniak[86], K. Wraight[59], J. Wu[14a,14e], M. Wu[64a], M. Wu[113], S.L. Wu[170], X. Wu[56], Y. Wu[62a], Z. Wu[135,62a], J. Wuerzinger[110], T.R. Wyatt[101], B.M. Wynne[52], S. Xella[42], L. Xia[14c], M. Xia[14b], J. Xiang[64c], X. Xiao[106], M. Xie[62a], X. Xie[62a], S. Xin[14a,14e], J. Xiong[17a], I. Xiotidis[146], D. Xu[14a], H. Xu[62a], H. Xu[62a], L. Xu[62a], R. Xu[128], T. Xu[106], Y. Xu[14b], Z. Xu[62b], Z. Xu[14a], B. Yabsley[147], S. Yacoob[33a], N. Yamaguchi[89], Y. Yamaguchi[154], H. Yamauchi[157], T. Yamazaki[17a], Y. Yamazaki[84], J. Yan[62c], S. Yan[126], Z. Yan[25], H.J. Yang[62c,62d], H.T. Yang[62a], S. Yang[62a], T. Yang[64c], X. Yang[62a], X. Yang[14a], Y. Yang[44], Y. Yang[62a], Z. Yang[62a,106], W-M. Yao[17a], Y.C. Yap[48], H. Ye[14c], H. Ye[55], J. Ye[44], S. Ye[29], X. Ye[62a], Y. Yeh[96], I. Yeletskikh[38], B.K. Yeo[17a], M.R. Yexley[91], P. Yin[41], K. Yorita[168], S. Younas[27b], C.J.S. Young[54], C. Young[143], Y. Yu[62a], M. Yuan[106], R. Yuan[62b,l], L. Yue[96], M. Zaazoua[35e], B. Zabinski[86], E. Zaid[52], T. Zakareishvili[149b], N. Zakharchuk[34], S. Zambito[56], J.A. Zamora Saa[137d,137b], J. Zang[153], D. Zanzi[54], O. Zaplatilek[132], C. Zeitnitz[171], H. Zeng[14a], J.C. Zeng[162], D.T. Zenger Jr[26], O. Zenin[37], T. Ženiš[28a], S. Zenz[94], S. Zerradi[35a], D. Zerwas[66], M. Zhai[14a,14e], B. Zhang[14c], D.F. Zhang[139], J. Zhang[62b], J. Zhang[6], K. Zhang[14a,14e], L. Zhang[14c], P. Zhang[14a,14e], R. Zhang[170], S. Zhang[106], T. Zhang[153], X. Zhang[62c], X. Zhang[62b], Y. Zhang[62c,5], Z. Zhang[17a], Z. Zhang[66], H. Zhao[138], P. Zhao[51], T. Zhao[62b], Y. Zhao[136], Z. Zhao[62a], A. Zhemchugov[38], K. Zheng[162], X. Zheng[62a], Z. Zheng[143], D. Zhong[162], B. Zhou[106], C. Zhou[170], H. Zhou[7], N. Zhou[62c], Y. Zhou[7], C.G. Zhu[62b], J. Zhu[106], Y. Zhu[62c], Y. Zhu[62a], X. Zhuang[14a], K. Zhukov[37], V. Zhulanov[37], N.I. Zimine[38], J. Zinsser[63b], M. Ziolkowski[141], L. Živković[15], A. Zoccoli[23b,23a], K. Zoch[56], T.G. Zorbas[139], O. Zormpa[46], W. Zou[41], L. Zwalinski[36]

[1] *Department of Physics, University of Adelaide, Adelaide; Australia*
[2] *Department of Physics, University of Alberta, Edmonton AB; Canada*
[3] (a) *Department of Physics, Ankara University, Ankara;* (b) *Division of Physics, TOBB University of Economics and Technology, Ankara; Türkiye*
[4] *LAPP, Université Savoie Mont Blanc, CNRS/IN2P3, Annecy; France*
[5] *APC, Université Paris Cité, CNRS/IN2P3, Paris; France*
[6] *High Energy Physics Division, Argonne National Laboratory, Argonne IL; United States of America*
[7] *Department of Physics, University of Arizona, Tucson AZ; United States of America*
[8] *Department of Physics, University of Texas at Arlington, Arlington TX; United States of America*
[9] *Physics Department, National and Kapodistrian University of Athens, Athens; Greece*
[10] *Physics Department, National Technical University of Athens, Zografou; Greece*
[11] *Department of Physics, University of Texas at Austin, Austin TX; United States of America*
[12] *Institute of Physics, Azerbaijan Academy of Sciences, Baku; Azerbaijan*
[13] *Institut de Física d'Altes Energies (IFAE), Barcelona Institute of Science and Technology, Barcelona; Spain*
[14] (a) *Institute of High Energy Physics, Chinese Academy of Sciences, Beijing;* (b) *Physics Department, Tsinghua University, Beijing;* (c) *Department of Physics, Nanjing University, Nanjing;* (d) *School of Science, Shenzhen Campus of Sun Yat-sen University;* (e) *University of Chinese Academy of Science (UCAS), Beijing; China*
[15] *Institute of Physics, University of Belgrade, Belgrade; Serbia*
[16] *Department for Physics and Technology, University of Bergen, Bergen; Norway*
[17] (a) *Physics Division, Lawrence Berkeley National Laboratory, Berkeley CA;* (b) *University of California, Berkeley CA; United States of America*
[18] *Institut für Physik, Humboldt Universität zu Berlin, Berlin; Germany*
[19] *Albert Einstein Center for Fundamental Physics and Laboratory for High Energy Physics, University of Bern, Bern; Switzerland*
[20] *School of Physics and Astronomy, University of Birmingham, Birmingham; United Kingdom*

[21] (a) Department of Physics, Bogazici University, Istanbul; (b) Department of Physics Engineering, Gaziantep University, Gaziantep; (c) Department of Physics, Istanbul University, Istanbul; (d) Istinye University, Sariyer, Istanbul; Türkiye
[22] (a) Facultad de Ciencias y Centro de Investigaciónes, Universidad Antonio Nariño, Bogotá; (b) Departamento de Física, Universidad Nacional de Colombia, Bogotá; Colombia
[23] (a) Dipartimento di Fisica e Astronomia A. Righi, Università di Bologna, Bologna; (b) INFN Sezione di Bologna; Italy
[24] Physikalisches Institut, Universität Bonn, Bonn; Germany
[25] Department of Physics, Boston University, Boston MA; United States of America
[26] Department of Physics, Brandeis University, Waltham MA; United States of America
[27] (a) Transilvania University of Brasov, Brasov; (b) Horia Hulubei National Institute of Physics and Nuclear Engineering, Bucharest; (c) Department of Physics, Alexandru Ioan Cuza University of Iasi, Iasi; (d) National Institute for Research and Development of Isotopic and Molecular Technologies, Physics Department, Cluj-Napoca; (e) University Politehnica Bucharest, Bucharest; (f) West University in Timisoara, Timisoara; (g) Faculty of Physics, University of Bucharest, Bucharest; Romania
[28] (a) Faculty of Mathematics, Physics and Informatics, Comenius University, Bratislava; (b) Department of Subnuclear Physics, Institute of Experimental Physics of the Slovak Academy of Sciences, Kosice; Slovak Republic
[29] Physics Department, Brookhaven National Laboratory, Upton NY; United States of America
[30] Universidad de Buenos Aires, Facultad de Ciencias Exactas y Naturales, Departamento de Física, y CONICET, Instituto de Física de Buenos Aires (IFIBA), Buenos Aires; Argentina
[31] California State University, CA; United States of America
[32] Cavendish Laboratory, University of Cambridge, Cambridge; United Kingdom
[33] (a) Department of Physics, University of Cape Town, Cape Town; (b) iThemba Labs, Western Cape; (c) Department of Mechanical Engineering Science, University of Johannesburg, Johannesburg; (d) National Institute of Physics, University of the Philippines Diliman (Philippines); (e) University of South Africa, Department of Physics, Pretoria; (f) University of Zululand, KwaDlangezwa; (g) School of Physics, University of the Witwatersrand, Johannesburg; South Africa
[34] Department of Physics, Carleton University, Ottawa ON; Canada
[35] (a) Faculté des Sciences Ain Chock, Réseau Universitaire de Physique des Hautes Energies - Université Hassan II, Casablanca; (b) Faculté des Sciences, Université Ibn-Tofail, Kénitra; (c) Faculté des Sciences Semlalia, Université Cadi Ayyad, LPHEA-Marrakech; (d) LPMR, Faculté des Sciences, Université Mohamed Premier, Oujda; (e) Faculté des sciences, Université Mohammed V, Rabat; (f) Institute of Applied Physics, Mohammed VI Polytechnic University, Ben Guerir; Morocco
[36] CERN, Geneva; Switzerland
[37] Affiliated with an institute covered by a cooperation agreement with CERN
[38] Affiliated with an international laboratory covered by a cooperation agreement with CERN
[39] Enrico Fermi Institute, University of Chicago, Chicago IL; United States of America
[40] LPC, Université Clermont Auvergne, CNRS/IN2P3, Clermont-Ferrand; France
[41] Nevis Laboratory, Columbia University, Irvington NY; United States of America
[42] Niels Bohr Institute, University of Copenhagen, Copenhagen; Denmark
[43] (a) Dipartimento di Fisica, Università della Calabria, Rende; (b) INFN Gruppo Collegato di Cosenza, Laboratori Nazionali di Frascati; Italy
[44] Physics Department, Southern Methodist University, Dallas TX; United States of America
[45] Physics Department, University of Texas at Dallas, Richardson TX; United States of America
[46] National Centre for Scientific Research "Demokritos", Agia Paraskevi; Greece
[47] (a) Department of Physics, Stockholm University; (b) Oskar Klein Centre, Stockholm; Sweden
[48] Deutsches Elektronen-Synchrotron DESY, Hamburg and Zeuthen; Germany
[49] Fakultät Physik, Technische Universität Dortmund, Dortmund; Germany
[50] Institut für Kern- und Teilchenphysik, Technische Universität Dresden, Dresden; Germany
[51] Department of Physics, Duke University, Durham NC; United States of America
[52] SUPA - School of Physics and Astronomy, University of Edinburgh, Edinburgh; United Kingdom
[53] INFN e Laboratori Nazionali di Frascati, Frascati; Italy
[54] Physikalisches Institut, Albert-Ludwigs-Universität Freiburg, Freiburg; Germany
[55] II. Physikalisches Institut, Georg-August-Universität Göttingen, Göttingen; Germany
[56] Département de Physique Nucléaire et Corpusculaire, Université de Genève, Genève; Switzerland
[57] (a) Dipartimento di Fisica, Università di Genova, Genova; (b) INFN Sezione di Genova; Italy
[58] II. Physikalisches Institut, Justus-Liebig-Universität Giessen, Giessen; Germany
[59] SUPA - School of Physics and Astronomy, University of Glasgow, Glasgow; United Kingdom
[60] LPSC, Université Grenoble Alpes, CNRS/IN2P3, Grenoble INP, Grenoble; France
[61] Laboratory for Particle Physics and Cosmology, Harvard University, Cambridge MA; United States of America
[62] (a) Department of Modern Physics and State Key Laboratory of Particle Detection and Electronics, University of Science and Technology of China, Hefei; (b) Institute of Frontier and Interdisciplinary Science and Key Laboratory of Particle Physics and Particle Irradiation (MOE), Shandong University, Qingdao; (c) School of Physics and Astronomy, Shanghai Jiao Tong University, Key Laboratory for Particle Astrophysics and Cosmology (MOE), SKLPPC, Shanghai; (d) Tsung-Dao Lee Institute, Shanghai; China
[63] (a) Kirchhoff-Institut für Physik, Ruprecht-Karls-Universität Heidelberg, Heidelberg; (b) Physikalisches Institut, Ruprecht-Karls-Universität Heidelberg, Heidelberg; Germany
[64] (a) Department of Physics, Chinese University of Hong Kong, Shatin, N.T., Hong Kong; (b) Department of Physics, University of Hong Kong, Hong Kong; (c) Department of Physics and Institute for Advanced Study, Hong Kong University of Science and Technology, Clear Water Bay, Kowloon, Hong Kong; China
[65] Department of Physics, National Tsing Hua University, Hsinchu; Taiwan
[66] IJCLab, Université Paris-Saclay, CNRS/IN2P3, 91405, Orsay; France
[67] Centro Nacional de Microelectrónica (IMB-CNM-CSIC), Barcelona; Spain
[68] Department of Physics, Indiana University, Bloomington IN; United States of America
[69] (a) INFN Gruppo Collegato di Udine, Sezione di Trieste, Udine; (b) ICTP, Trieste; (c) Dipartimento Politecnico di Ingegneria e Architettura, Università di Udine, Udine; Italy
[70] (a) INFN Sezione di Lecce; (b) Dipartimento di Matematica e Fisica, Università del Salento, Lecce; Italy
[71] (a) INFN Sezione di Milano; (b) Dipartimento di Fisica, Università di Milano, Milano; Italy
[72] (a) INFN Sezione di Napoli; (b) Dipartimento di Fisica, Università di Napoli, Napoli; Italy
[73] (a) INFN Sezione di Pavia; (b) Dipartimento di Fisica, Università di Pavia, Pavia; Italy
[74] (a) INFN Sezione di Pisa; (b) Dipartimento di Fisica E. Fermi, Università di Pisa, Pisa; Italy
[75] (a) INFN Sezione di Roma; (b) Dipartimento di Fisica, Sapienza Università di Roma, Roma; Italy
[76] (a) INFN Sezione di Roma Tor Vergata; (b) Dipartimento di Fisica, Università di Roma Tor Vergata, Roma; Italy
[77] (a) INFN Sezione di Roma Tre; (b) Dipartimento di Matematica e Fisica, Università Roma Tre, Roma; Italy
[78] (a) INFN-TIFPA; (b) Università degli Studi di Trento, Trento; Italy
[79] Universität Innsbruck, Department of Astro and Particle Physics, Innsbruck; Austria
[80] University of Iowa, Iowa City IA; United States of America
[81] Department of Physics and Astronomy, Iowa State University, Ames IA; United States of America
[82] (a) Departamento de Engenharia Elétrica, Universidade Federal de Juiz de Fora (UFJF), Juiz de Fora; (b) Universidade Federal do Rio De Janeiro COPPE/EE/IF, Rio de Janeiro; (c) Instituto de Física, Universidade de São Paulo, São Paulo; (d) Rio de Janeiro State University, Rio de Janeiro; Brazil
[83] KEK, High Energy Accelerator Research Organization, Tsukuba; Japan
[84] Graduate School of Science, Kobe University, Kobe; Japan
[85] (a) AGH University of Krakow, Faculty of Physics and Applied Computer Science, Krakow; (b) Marian Smoluchowski Institute of Physics, Jagiellonian University, Krakow; Poland
[86] Institute of Nuclear Physics Polish Academy of Sciences, Krakow; Poland
[87] Faculty of Science, Kyoto University, Kyoto; Japan
[88] Kyoto University of Education, Kyoto; Japan

[89] Research Center for Advanced Particle Physics and Department of Physics, Kyushu University, Fukuoka; Japan
[90] Instituto de Física La Plata, Universidad Nacional de La Plata and CONICET, La Plata; Argentina
[91] Physics Department, Lancaster University, Lancaster; United Kingdom
[92] Oliver Lodge Laboratory, University of Liverpool, Liverpool; United Kingdom
[93] Department of Experimental Particle Physics, Jožef Stefan Institute and Department of Physics, University of Ljubljana, Ljubljana; Slovenia
[94] School of Physics and Astronomy, Queen Mary University of London, London; United Kingdom
[95] Department of Physics, Royal Holloway University of London, Egham; United Kingdom
[96] Department of Physics and Astronomy, University College London, London; United Kingdom
[97] Louisiana Tech University, Ruston LA; United States of America
[98] Fysiska institutionen, Lunds universitet, Lund; Sweden
[99] Departamento de Física Teorica C-15 and CIAFF, Universidad Autónoma de Madrid, Madrid; Spain
[100] Institut für Physik, Universität Mainz, Mainz; Germany
[101] School of Physics and Astronomy, University of Manchester, Manchester; United Kingdom
[102] CPPM, Aix-Marseille Université, CNRS/IN2P3, Marseille; France
[103] Department of Physics, University of Massachusetts, Amherst MA; United States of America
[104] Department of Physics, McGill University, Montreal QC; Canada
[105] School of Physics, University of Melbourne, Victoria; Australia
[106] Department of Physics, University of Michigan, Ann Arbor MI; United States of America
[107] Department of Physics and Astronomy, Michigan State University, East Lansing MI; United States of America
[108] Group of Particle Physics, University of Montreal, Montreal QC; Canada
[109] Fakultät für Physik, Ludwig-Maximilians-Universität München, München; Germany
[110] Max-Planck-Institut für Physik (Werner-Heisenberg-Institut), München; Germany
[111] Graduate School of Science and Kobayashi-Maskawa Institute, Nagoya University, Nagoya; Japan
[112] Department of Physics and Astronomy, University of New Mexico, Albuquerque NM; United States of America
[113] Institute for Mathematics, Astrophysics and Particle Physics, Radboud University/Nikhef, Nijmegen; Netherlands
[114] Nikhef National Institute for Subatomic Physics and University of Amsterdam, Amsterdam; Netherlands
[115] Department of Physics, Northern Illinois University, DeKalb IL; United States of America
[116] (a) New York University Abu Dhabi, Abu Dhabi; (b) University of Sharjah, Sharjah; United Arab Emirates
[117] Department of Physics, New York University, New York NY; United States of America
[118] Ochanomizu University, Otsuka, Bunkyo-ku, Tokyo; Japan
[119] Ohio State University, Columbus OH; United States of America
[120] Homer L. Dodge Department of Physics and Astronomy, University of Oklahoma, Norman OK; United States of America
[121] Department of Physics, Oklahoma State University, Stillwater OK; United States of America
[122] Palacký University, Joint Laboratory of Optics, Olomouc; Czech Republic
[123] Institute for Fundamental Science, University of Oregon, Eugene, OR; United States of America
[124] Graduate School of Science, Osaka University, Osaka; Japan
[125] Department of Physics, University of Oslo, Oslo; Norway
[126] Department of Physics, Oxford University, Oxford; United Kingdom
[127] LPNHE, Sorbonne Université, Université Paris Cité, CNRS/IN2P3, Paris; France
[128] Department of Physics, University of Pennsylvania, Philadelphia PA; United States of America
[129] Department of Physics and Astronomy, University of Pittsburgh, Pittsburgh PA; United States of America
[130] (a) Laboratório de Instrumentação e Física Experimental de Partículas - LIP, Lisboa; (b) Departamento de Física, Faculdade de Ciências, Universidade de Lisboa, Lisboa; (c) Departamento de Física, Universidade de Coimbra, Coimbra; (d) Centro de Física Nuclear da Universidade de Lisboa, Lisboa; (e) Departamento de Física, Universidade do Minho, Braga; (f) Departamento de Física Teórica y del Cosmos, Universidad de Granada, Granada (Spain); (g) Departamento de Física, Instituto Superior Técnico, Universidade de Lisboa, Lisboa; Portugal
[131] Institute of Physics of the Czech Academy of Sciences, Prague; Czech Republic
[132] Czech Technical University in Prague, Prague; Czech Republic
[133] Charles University, Faculty of Mathematics and Physics, Prague; Czech Republic
[134] Particle Physics Department, Rutherford Appleton Laboratory, Didcot; United Kingdom
[135] IRFU, CEA, Université Paris-Saclay, Gif-sur-Yvette; France
[136] Santa Cruz Institute for Particle Physics, University of California Santa Cruz, Santa Cruz CA; United States of America
[137] (a) Departamento de Física, Pontificia Universidad Católica de Chile, Santiago; (b) Millennium Institute for Subatomic physics at high energy frontier (SAPHIR), Santiago; (c) Instituto de Investigación Multidisciplinario en Ciencia y Tecnología, y Departamento de Física, Universidad de La Serena; (d) Universidad Andres Bello, Department of Physics, Santiago; (e) Instituto de Alta Investigación, Universidad de Tarapacá, Arica; (f) Departamento de Física, Universidad Técnica Federico Santa María, Valparaíso; Chile
[138] Department of Physics, University of Washington, Seattle WA; United States of America
[139] Department of Physics and Astronomy, University of Sheffield, Sheffield; United Kingdom
[140] Department of Physics, Shinshu University, Nagano; Japan
[141] Department Physik, Universität Siegen, Siegen; Germany
[142] Department of Physics, Simon Fraser University, Burnaby BC; Canada
[143] SLAC National Accelerator Laboratory, Stanford CA; United States of America
[144] Department of Physics, Royal Institute of Technology, Stockholm; Sweden
[145] Departments of Physics and Astronomy, Stony Brook University, Stony Brook NY; United States of America
[146] Department of Physics and Astronomy, University of Sussex, Brighton; United Kingdom
[147] School of Physics, University of Sydney, Sydney; Australia
[148] Institute of Physics, Academia Sinica, Taipei; Taiwan
[149] (a) E. Andronikashvili Institute of Physics, Iv. Javakhishvili Tbilisi State University, Tbilisi; (b) High Energy Physics Institute, Tbilisi State University, Tbilisi; (c) University of Georgia, Tbilisi; Georgia
[150] Department of Physics, Technion, Israel Institute of Technology, Haifa; Israel
[151] Raymond and Beverly Sackler School of Physics and Astronomy, Tel Aviv University, Tel Aviv; Israel
[152] Department of Physics, Aristotle University of Thessaloniki, Thessaloniki; Greece
[153] International Center for Elementary Particle Physics and Department of Physics, University of Tokyo, Tokyo; Japan
[154] Department of Physics, Tokyo Institute of Technology, Tokyo; Japan
[155] Department of Physics, University of Toronto, Toronto ON; Canada
[156] (a) TRIUMF, Vancouver BC; (b) Department of Physics and Astronomy, York University, Toronto ON; Canada
[157] Division of Physics and Tomonaga Center for the History of the Universe, Faculty of Pure and Applied Sciences, University of Tsukuba, Tsukuba; Japan
[158] Department of Physics and Astronomy, Tufts University, Medford MA; United States of America
[159] United Arab Emirates University, Al Ain; United Arab Emirates
[160] Department of Physics and Astronomy, University of California Irvine, Irvine CA; United States of America
[161] Department of Physics and Astronomy, University of Uppsala, Uppsala; Sweden
[162] Department of Physics, University of Illinois, Urbana IL; United States of America
[163] Instituto de Física Corpuscular (IFIC), Centro Mixto Universidad de Valencia - CSIC, Valencia; Spain

[164] *Department of Physics, University of British Columbia, Vancouver BC; Canada*
[165] *Department of Physics and Astronomy, University of Victoria, Victoria BC; Canada*
[166] *Fakultät für Physik und Astronomie, Julius-Maximilians-Universität Würzburg, Würzburg; Germany*
[167] *Department of Physics, University of Warwick, Coventry; United Kingdom*
[168] *Waseda University, Tokyo; Japan*
[169] *Department of Particle Physics and Astrophysics, Weizmann Institute of Science, Rehovot; Israel*
[170] *Department of Physics, University of Wisconsin, Madison WI; United States of America*
[171] *Fakultät für Mathematik und Naturwissenschaften, Fachgruppe Physik, Bergische Universität Wuppertal, Wuppertal; Germany*
[172] *Department of Physics, Yale University, New Haven CT; United States of America*

[a] Also Affiliated with an institute covered by a cooperation agreement with CERN.
[b] Also at An-Najah National University, Nablus; Palestine.
[c] Also at Borough of Manhattan Community College, City University of New York, New York NY; United States of America.
[d] Also at Bruno Kessler Foundation, Trento; Italy.
[e] Also at Center for High Energy Physics, Peking University; China.
[f] Also at Center for Interdisciplinary Research and Innovation (CIRI-AUTH), Thessaloniki; Greece.
[g] Also at Centro Studi e Ricerche Enrico Fermi; Italy.
[h] Also at CERN, Geneva; Switzerland.
[i] Also at Département de Physique Nucléaire et Corpusculaire, Université de Genève, Genève; Switzerland.
[j] Also at Departament de Fisica de la Universitat Autonoma de Barcelona, Barcelona; Spain.
[k] Also at Department of Financial and Management Engineering, University of the Aegean, Chios; Greece.
[l] Also at Department of Physics and Astronomy, Michigan State University, East Lansing MI; United States of America.
[m] Also at Department of Physics, Ben Gurion University of the Negev, Beer Sheva; Israel.
[n] Also at Department of Physics, California State University, East Bay; United States of America.
[o] Also at Department of Physics, California State University, Sacramento; United States of America.
[p] Also at Department of Physics, King’s College London, London; United Kingdom.
[q] Also at Department of Physics, Stanford University, Stanford CA; United States of America.
[r] Also at Department of Physics, University of Fribourg, Fribourg; Switzerland.
[s] Also at Department of Physics, University of Thessaly; Greece.
[t] Also at Department of Physics, Westmont College, Santa Barbara; United States of America.
[u] Also at Hellenic Open University, Patras; Greece.
[v] Also at Institucio Catalana de Recerca i Estudis Avancats, ICREA, Barcelona; Spain.
[w] Also at Institut für Experimentalphysik, Universität Hamburg, Hamburg; Germany.
[x] Also at Institute for Nuclear Research and Nuclear Energy (INRNE) of the Bulgarian Academy of Sciences, Sofia; Bulgaria.
[y] Also at Institute of Applied Physics, Mohammed VI Polytechnic University, Ben Guerir; Morocco.
[z] Also at Institute of Particle Physics (IPP); Canada.
[aa] Also at Institute of Physics and Technology, Ulaanbaatar; Mongolia.
[ab] Also at Institute of Physics, Azerbaijan Academy of Sciences, Baku; Azerbaijan.
[ac] Also at Institute of Theoretical Physics, Ilia State University, Tbilisi; Georgia.
[ad] Also at L2IT, Université de Toulouse, CNRS/IN2P3, UPS, Toulouse; France.
[ae] Also at Lawrence Livermore National Laboratory, Livermore; United States of America.
[af] Also at National Institute of Physics, University of the Philippines Diliman (Philippines); Philippines.
[ag] Also at Technical University of Munich, Munich; Germany.
[ah] Also at The Collaborative Innovation Center of Quantum Matter (CICQM), Beijing; China.
[ai] Also at TRIUMF, Vancouver BC; Canada.
[aj] Also at Università di Napoli Parthenope, Napoli; Italy.
[ak] Also at University of Colorado Boulder, Department of Physics, Colorado; United States of America.
[al] Also at Washington College, Maryland; United States of America.
[am] Also at Yeditepe University, Physics Department, Istanbul; Türkiye.
* Deceased.